

**REPUBLIC OF TURKEY
HACETTEPE UNIVERSITY
FACULTY OF HEALTH SCIENCES**

**IMMUNOMODULATORY EFFECTS OF NOVEL IMMUNE COSTIMULATOR SA-4-1BBL
IN NNK-INDUCED LUNG CANCER PRECLINICAL MODEL**

Ayşe Ece GÜLEN MD, PhD

TUMOR BIOLOGY AND IMMUNOLOGY PROGRAM

DOCTOR OF PHILOSOPHY THESIS

ANKARA

2024

**REPUBLIC OF TURKEY
HACETTEPE UNIVERSITY
FACULTY OF HEALTH SCIENCES**

**IMMUNOMODULATORY EFFECTS OF NOVEL IMMUNE COSTIMULATOR SA-4-1BBL
IN NNK-INDUCED LUNG CANCER PRECLINICAL MODEL**

Ayşe Ece GÜLEN MD, PhD

**TUMOR BIOLOGY AND IMMUNOLOGY PROGRAM
DOCTOR OF PHILOSOPHY THESIS**

Advisor of Thesis

Assoc. Prof. Dr. Hande CANPINAR

ANKARA

2024



**IMMUNOMODULATORY EFFECTS OF NOVEL IMMUNE COSTIMULATOR SA-4-1BBL
IN NNK-INDUCED LUNG CANCER PRECLINICAL MODEL**

AYŞE ECE GÜLEN

Supervisor: Assoc. Prof. Hande CANPINAR, PhD

This thesis study has been approved and accepted as a PhD dissertation in the “Tumor Biology and Immunology Program” by the assessment committee, whose members are listed below, on June 13, 2024.

Chairman of the Committee: Prof. Dr. Bilkay BAŞTÜRK, MD.PhD
Başkent University

Member: Prof.Dr. Deniz ÇAĞDAŞ AYVAZ, MD.PhD
Hacettepe University

Member: Prof.Dr. Resul KARAKUŞ, MD.PhD
Gazi University

Member: Assoc. Prof. Neşe ÜNVER, PhD
Hacettepe University

Member: Assoc. Prof. Sevil Oskay HALAÇLI, MD
Hacettepe University

This dissertation has been approved by the above committee in conformity to the related issues of Hacettepe University Graduate Education and Examination Regulation.

Prof. Müge YEMİŞÇİ ÖZKAN, MD, PhD

Director

09/07/2024

YAYIMLAMA VE FİKRİ MÜLKİYET HAKLARI BEYANI

Enstitü tarafından onaylanan lisansüstü tezimin/raporumun tamamını veya herhangi bir kısmını, basılı (kağıt) ve elektronik formatta arşivleme ve aşağıda verilen koşullarla kullanıma açma iznini Hacettepe Üniversitesine verdiğimi bildiririm. Bu izinle Üniversiteye verilen kullanım hakları dışındaki tüm fikri mülkiyet haklarım bende kalacak, tezimin tamamının ya da bir bölümünün gelecekteki çalışmalarda (makale, kitap, lisans ve patent vb.) kullanım hakları bana ait olacaktır.

Tezin kendi orijinal çalışmam olduğunu, başkalarının haklarını ihlal etmediğimi ve tezimin tek yetkili sahibi olduğumu beyan ve taahhüt ederim. Tezimde yer alan telif hakkı bulunan ve sahiplerinden yazılı izin alınarak kullanılması zorunlu metinlerin yazılı izin alınarak kullandığımı ve istenildiğinde suretlerini Üniversiteye teslim etmeyi taahhüt ederim.

Yükseköğretim Kurulu tarafından yayınlanan “Lisansüstü Tezlerin Elektronik Ortamda Toplanması, Düzenlenmesi ve Erişime Açılmasına İlişkin Yönerge” kapsamında tezim aşağıda belirtilen koşullar haricince YÖK Ulusal Tez Merkezi / H.Ü. Kütüphaneleri Açık Erişim Sisteminde erişime açılır.

- Enstitü / Fakülte yönetim kurulu kararı ile tezimin erişime açılması mezuniyet tarihimden itibaren 2 yıl ertelenmiştir. (1)
- Enstitü / Fakülte yönetim kurulunun gerekçeli kararı ile tezimin erişime açılması mezuniyet tarihimden itibaren ... ay ertelenmiştir. (2)
- Tezimle ilgili gizlilik kararı verilmiştir. (3)

11 /07/2024

Ayşe Ece GÜLEN

i i“Lisansüstü Tezlerin Elektronik Ortamda Toplanması, Düzenlenmesi ve Erişime Açılmasına İlişkin Yönerge”

(1) Madde 6. 1. Lisansüstü teze ilgili patent başvurusu yapılması veya patent alma sürecinin devam etmesi durumunda, tez danışmanının önerisi ve enstitü anabilim dalının uygun görüşü üzerine enstitü veya fakülte yönetim kurulu iki yıl süre ile tezin erişime açılmasının ertelenmesine karar verebilir.

(2) Madde 6. 2. Yeni teknik, materyal ve metodların kullanıldığı, henüz makaleye dönüşmemiş veya patent gibi yöntemlerle korunmamış ve internetten paylaşılması durumunda 3. şahıslara veya kurumlara haksız kazanç imkanı oluşturabilecek bilgi ve bulguları içeren tezler hakkında tez danışmanının önerisi ve enstitü anabilim dalının uygun görüşü üzerine enstitü veya fakülte yönetim kurulunun gerekçeli kararı ile altı ayı aşmamak üzere tezin erişime açılması engellenebilir.

(3) Madde 7. 1. Ulusal çıkarları veya güvenliği ilgilendiren, emniyet, istihbarat, savunma ve güvenlik, sağlık vb. konulara ilişkin lisansüstü tezlerle ilgili gizlilik kararı, tezin yapıldığı kurum tarafından verilir *. Kurum ve kuruluşlarla yapılan işbirliği protokolü çerçevesinde hazırlanan lisansüstü tezlere ilişkin gizlilik kararı ise, ilgili kurum ve kuruluşun önerisi ile enstitü veya fakültenin uygun görüşü üzerine üniversite yönetim kurulu tarafından verilir. Gizlilik kararı verilen tezler Yükseköğretim Kuruluna bildirilir. Madde 7.2. Gizlilik kararı verilen tezler gizlilik süresince enstitü veya fakülte tarafından gizlilik kuralları çerçevesinde muhafaza edilir, gizlilik kararının kaldırılması halinde Tez Otomasyon Sistemine yüklenir * Tez danışmanının önerisi ve enstitü anabilim dalının uygun görüşü üzerine enstitü veya fakülte yönetim kurulu tarafından karar verilir.

ETHICAL DECLARATION

In this thesis study, I declare that all the information and documents have been obtained in the base of the academic rules and all audio-visual and written information and results have been presented according to the rules of scientific ethics. I did not do any distortion in the data set. In the case of using other works, related studies have been fully cited in accordance with the scientific standards. I also declare that my thesis study is original except for cited references. It was produced by me in consultation with supervisor Dr. Esmâ Yolcu and Assoc. Prof. Dr. Hande Canpınar and written according to the rules of thesis writing of Hacettepe University Institute of Health Sciences

11/07/2024

Ayşe Ece GÜLEN

ACKNOWLEDGEMENTS

My deepest gratitude goes to my advisor, Dr. Hande CANPINAR, for her exceptional mentorship, profound wisdom, and unwavering belief in me in my journey. Also, I owe a debt of gratitude to Dr. Esmâ YOLCU and Dr. Haval SHIRWAN, who not only provided me with the opportunity in their laboratory to conduct my doctoral research but also offered boundless guidance and support. Dr. Esmâ YOLCU illuminated the challenging period I spent away from my homeland with mentorship, unwavering belief in me, and invaluable advice. I also appreciate my former advisor, Dr. Grcan GNAYDIN, your journey has inspired me, and I appreciate your contributions to my journey.

My deepest appreciation extends to my previous and current committee members, for their invaluable guidance and insightful feedback.

To my colleagues from Yolcu/ Shirwan/ Gomez laboratory, your collaborative spirit, and diverse perspectives have fostered an environment for me to develop my scientific perspectives and taught me how to work as a team.

I owe an immeasurable gratitude to my family whose unwavering love, support, and sacrifice have been the bedrock of my medical school and doctoral journey. You always believe in me, encourage me during my moments of doubt, and celebrate my big and small milestones. Your sacrifices and support have been my greatest source of strength and motivation.

To my friends, in Trkiye and the United States, who have always stood by me with support, understanding, and encouragement, I am deeply grateful. Your presence in laughter, or the worst days has provided solace and joy amidst the rigors of academia and the challenges of medical school.

To the countless individuals whose names may not appear on these pages but whose contributions have left a mark on this work, I offer my heartfelt thanks.

Lastly, I deem it a duty to commemorate Mustafa Kemal Atatrk respectfully and gratefully, who paved the way for the establishment and resurgence of our nation, and who will always remain the greatest guiding light for me.

"Dinlenmemek zere yola ıkanlar asla yorulmazlar."

ABSTRACT

Gulen, A.E., Immunomodulatory Effects of Novel Immune Costimulator SA-4-1BBL in NNK Induced Lung Cancer Preclinical Model, Hacettepe University Graduate School Health Sciences Basic Oncology Department of Tumor Biology and Immunology Philosophy Thesis, Ankara, 2024. Immune checkpoint inhibitors hold promise in treating various malignancies, but their use is limited due to side effects and treatment resistance. Therefore, the immune costimulation pathway is an important target to enhance immune responses and overcome immune suppression in cancer immunotherapy. 4-1BB (CD137) is a potent molecule that initiates a costimulatory signal in the 4-1BB/4-1BBL pathway, making it a promising candidate for new therapeutic approaches that can be developed in the clinic. 4-1BB, also known as TNFR-9, is a costimulatory molecule belonging to the TNFR superfamily. The 4-1BB receptor is not continuously expressed on immune cells; its expression begins with immune activation of the cells. It is expressed in T cells, natural killer cells, and B cells, enhancing their survival and functionality. 4-1BBL is a protein that is functional only in its soluble form. Preclinical studies in mice after cloning the natural ligand for CD137 have shown that 4-1BBL provides therapeutic benefits in various solid and hematological malignancies. Agonistic 4-1BB antibodies have been used in both preclinical and clinical studies, but their application has been hindered due to reported hepatotoxicity. This limitation presents challenges for the broader clinical adoption of approaches involving agonistic 4-1BB monoclonal antibodies. Therefore, in this thesis, an alternative structure of the 4-1BBL protein has been designed. The recombinant form of the 4-1BBL protein was produced by fusing the extracellular segments of mouse 4-1BBL with streptavidin.

In this thesis study, during the first 8 weeks, NNK, the most potent carcinogen in tobacco, was administered intraperitoneally to A/J mice weekly to induce lung cancer. To investigate the immunomodulatory effects of SA-4-1BBL, mice were injected subcutaneously with 100 µg SA-4-1BBL in the sixth and eighth weeks. The mice were observed for toxicity and side effects during an 18-week follow-up through their body weights and general examinations. Under the same conditions of NNK and SA-4-1BBL administration, some mice were separated, and *in vivo* depletion of different immune cell populations was performed. Depletion antibodies with *in vivo* activity and reactivity for CD4⁺, CD8⁺ T lymphocytes, and NK cells were administered intraperitoneally to the depletion group animals in the sixth and eighth weeks of NNK injections. The animals were monitored for clinical status and body weights to investigate possible side effects of *in vivo* depletion antibodies. *In vivo* cell depletion was observed to create no differences among experimental groups. The doses of *in vivo* depletion antibodies used were sufficient to cause depletion of CD4 and CD8

lymphocytes. At the end of the 18th week, the mice were sacrificed, and their lungs were evaluated for macroscopic and microscopic tumor formation. In this evaluation, it was observed that the number of macroscopic and microscopic tumors in the lung tissues of the mice treated with SA-4-1BBL was significantly reduced compared to the control group that did not receive the treatment. In vivo depletion of CD4⁺, CD8⁺ T lymphocytes, and NK cells abolished the protective effect of SA-4-1BBL monotherapy. A significant increase in macroscopic and microscopic tumor nodule formation was observed in the group with depleted CD4⁺ T cells. In vivo depletion of CD8⁺ T lymphocytes and NK cells resulted in a marked increase in microscopic tumor nodule formation, but no significant change was observed in macroscopic tumor nodule formation. These findings suggest that CD4⁺ T lymphocytes are essential for establishing an antitumor immune response, which aligns with a previous study using SA-4-1BBL. Given the nature of carcinogen-induced cancer models, it is possible to form metastases or tumor foci in different organs. Therefore, the mice were thoroughly evaluated on the termination day, and all organ systems were checked for metastases and tumor formation. Interestingly, one mouse in the in vivo CD4⁺ T lymphocyte depletion group showed a metastatic mass near the mandible. This lesion was also removed on the termination day and tissue was collected for histopathological analysis. The analyses showed that this lesion was metastatic and had the same histopathological phenotype as the nodules observed in the lungs. In flow cytometry analysis of leukocytes infiltrating the tumor, the mass showed a 14-fold increase in PD1⁺ CD4⁺ T lymphocytes and PD1⁺ CD8⁺ T lymphocytes (PD-1, programmed cell death protein 1) compared to the lungs with microscopic tumor nodules. Additionally, in vivo depletion of CD8⁺ T lymphocytes significantly reduced the protective effect of SA-4-1BBL monotherapy. The microscopic tumor nodules in mice treated with SA-4-1BBL but depleted of T lymphocytes or NK cells were significantly larger compared to the NNK control under comparable conditions. These data indicate that the immunotherapeutic efficacy of SA-4-1BBL relies on the presence of T lymphocytes and NK cells. Furthermore, lungs and lung-draining lymph nodes were collected and processed for detailed immunophenotyping to isolate immune cells infiltrating the tissue and compare differences in immune cell populations among different treatment groups. Compared to the control group (NNK + saline), it was shown that SA-4-1BBL significantly increased the absolute number of CD4⁺ central memory T cells (CD4⁺CD44^{high}CD62L^{high}) in the lungs and lung-draining lymph nodes ($p < 0.05$). The number of naive CD4⁺ T lymphocytes (CD4⁺CD44^{low}CD62L^{high}) in the lung-draining lymph nodes of the SA-4-1BBL treatment group was significantly higher compared to the control group. Moreover, in the lung-draining lymph nodes of animals treated with SA-4-1BBL, a significant decrease was observed in the absolute number of PD-1⁺ CD8⁺ T lymphocytes due to the immunomodulatory effect of SA-4-1BBL. The programmed cell death protein 1

(PD-1) receptor is a critical immune checkpoint receptor primarily expressed on the cell membranes of activated T cells. PD-1/PD-L1 binding provides inhibitory signals that reduce immune activation. The decrease in PD-1+ CD8+ T lymphocytes in the SA-4-1BBL treatment group may serve as an additional mechanism to support its antitumoral immunomodulatory effect.

Our study results observed that SA-4-1BBL treatment suppressed lung cancer development. T lymphocytes and NK (natural killer) cells played a significant role in this suppression. In vivo depletion of these immune cells was shown to be responsible for reducing the antitumoral protective effect of SA-4-1BBL. Our thesis study results suggest that SA-4-1BBL, an immune checkpoint stimulator, is a candidate that can create a protective immune response as a single agent in a chemically induced preclinical lung cancer model.

Keywords: 4-1BB, cancer immunotherapy, lung cancer, NNK, immunomodulation

Supported by: This thesis project was funded by the U.S. Department of Defense.

ÖZET

GÜLEN, A.E., İmmün Kostimülatör SA-4-1BBL'nin NNK ile İndüklenmiş Akciğer Kanseri Preklinik Modelindeki İmmünomodülatör Etkileri, Hacettepe Üniversitesi Sağlık Bilimleri Enstitüsü, Temel Onkoloji Bilim Dalı Tümör Biyolojisi ve İmmünolojisi Programı Doktora Tezi, Ankara, 2024. İmmün kontrol noktası inhibitörleri, farklı malignitelerin tedavisinde umut vericidir ancak kullanımları, yan etkileri ve tedavi direnci nedeniyle kısıtlıdır. Bu nedenle immün kostimülasyon yoluyla immün yanıtları arttırmak ve kanser immünoterapisindeki immün baskılamanın üstesinden gelinmesi açısından önemli bir hedef olarak bulunmaktadır. 4-1BB (CD137), 4-1BB/ 4-1BBL yoluyla kostimülatör sinyali başlatan etkili bir moleküldür. Bu nedenle klinikte geliştirilebilecek yeni tedavi yaklaşımları için de iyi bir adaydır. 4-1BB, TNFR super ailesine ait bir kostimülatör moleküldür ve TNFR-9 olarak da adlandırılmaktadır. 4-1BB reseptörü, immün hücrelerde devamlı ifade edilmez, ifadesi hücrelerin immün aktivasyonu ile başlar. T hücreler, doğal öldürücü hücreler ve B hücrelerde ifade edilerek sağkalımlarını ve işlevselliklerini artırıcı etkide bulunur. 4-1BBL, yalnızca çözünür formunda işlevsel olan bir proteindir. CD137 için doğal ligandın klonlanması sonrası farelerde yapılan ön klinik çalışmalar, 4-1BBL'nin çeşitli solid ve hematolojik malignitelerde terapötik faydalar sağladığını göstermiştir. Agonistik 4-1BB antikoru hem ön klinik çalışmalarda hem de klinik çalışmalarda kullanılmıştır, ancak uygulamaları bildirilen hepatotoksisite nedeniyle engellenmiştir. Bu kısıtlama, agonistik 4-1BB monoklonal antikoru içeren yaklaşımların klinik olarak daha geniş çapta benimsenmesi için zorluklar oluşturur. Bu nedenle, bu tez çalışmasında alternatif bir yapıda olan 4-1BBL proteini tasarlanmıştır. 4-1BBL proteininin rekombinant formu fare 4-1BBL'nin hücre dışı bölümlerinin streptavidinle birleştirilmesiyle üretilmiştir. Bu tez çalışmasında, ilk 8 hafta boyunca tütünün en potent karsinojeni olan NNK, akciğer kanserini A/J farelerde oluşturmak için haftalık olarak intraperitoneal yolla farelere verilmiştir. SA-4-1BBL'nin immünomodülatör etkilerini incelemek için de fareler, altıncı ve sekizinci haftalarda 100 µg subkutan SA-4-1BBL ile enjekte edilmiştir. Fareler, 18 haftalık takipleri süresince vücut ağırlıkları ve genel muayeneleriyle toksisite ve yan etki oluşumu açısından gözlenmiştir. NNK ve SA-4-1BBL uygulamasının aynı koşulları altında, bazı fareler ayrıldı ve farklı immün hücre popülasyonlarının in vivo baskılanması gerçekleştirildi. CD4+, CD8+ T lenfositler ve NK hücre popülasyonları için in vivo aktivite ve reaktiviteye sahip depresyon antikoru, NNK enjeksiyonlarının altıncı ve sekizinci haftalarında intraperitoneal enjeksiyon yoluyla baskılanma grubu hayvanlarına aynı anda uygulandı. Olası in vivo baskılayıcı antikor yan etkilerini araştırmak için hayvanlar klinik durumları ve vücut ağırlıkları kullanılarak izlendi. In vivo hücre baskılanması, deneysel gruplar arasında herhangi bir farklılık oluşturmadığı gözlemlendi. Kullanılan in vivo baskılayıcı antikor dozlarının, CD4 ve CD8 lenfosit baskılanmasına neden olacak kadar yeterli olduğu

görüldü. 18. haftanın sonunda, fareler sakrifiye edildi ve akciğerleri makroskopik ve mikroskopik tümör oluşumu açısından değerlendirildi. Bu değerlendirmede, SA-4-1BBL tedavisi alan farelerin akciğer dokularında, tedavi almayan kontrol grubuna göre anlamlı derecede makroskopik ve mikroskopik tümör sayılarının azalmış olduğu görülmüştür. CD4+, CD8+ T lenfositler ve NK hücrelerinin in vivo baskılanması, SA-4-1BBL monoterapisinin koruyucu etkisini ortadan kaldırmıştır. CD4+ T hücreleri baskılanmış grupta, makroskopik ve mikroskopik tümör nodül oluşumunda anlamlı bir artış görüldü. CD8+ T lenfositlerinin ve NK hücrelerinin in vivo baskılanımı, mikroskopik tümör nodül oluşumunda belirgin bir artışa neden oldu, ancak makroskopik tümör nodül oluşumunda anlamlı bir değişiklik gözlenmedi. Bu bulgular, CD4+ T lenfositlerin antitümöral bağışıklık yanıtını oluşturmak için esas olduğunu ve bu bulgunun SA-4-1BBL kullanılarak yapılan geçmiş bir çalışmayla paralel olduğunu öne sürmektedir. Kanserojenle indüklenen kanser modellerinin doğası gereği, farklı organlarda metastaz veya tümör odağı oluşumu mümkündür. Bu nedenle, sonlandırma gününde fareler detaylı bir şekilde değerlendirildi ve tüm organ sistemleri metastaz ve tümör oluşumu açısından kontrol edildi. İlginç bir bulgu olarak, in vivo CD4+ T lenfositler baskılanan gruptaki bir fare, mandibula yakınında metastatik bir kitle odağı gösterdi. Sonlandırma gününde bu lezyon da çıkarıldı ve histopatolojik analizler için doku toplandı. Analizler, bu lezyonun metastatik olduğunu ve akciğerlerde gözlemlenen nodüllerle aynı histopatolojik fenotipe sahip olduğunu gösterdi. Tümörü infiltre eden lökositlerin akım sitometrisi analizinde, kitle, mikroskopik tümör nodülleri olan akciğerlere göre PD1+ CD4+ T lenfositleri ve PD1+ CD8+ T lenfositlerinde (PD-1, programlanmış hücre ölüm protein 1) 14 kat artış gösterdi. Ayrıca, in vivo CD8+ T lenfosit baskılanımı, SA-4-1BBL monoterapisinin koruyucu etkisinde belirgin bir azalmaya neden oldu. SA-4-1BBL tedavisi alan farelerle karşılaştırıldığında, SA-4-1BBL uygulanmış ancak T lenfositleri veya NK hücreleri baskılanmış olan farelerdeki mikroskopik tümör nodülleri, NNK kontrolü ile karşılaştırılabilir şekilde anlamlı derecede daha büyük boyutlara sahipti. Bu veriler, SA-4-1BBL'nin immünoterapötik etkinliğinin T lenfositler ve NK hücrelerinin varlığına dayandığını işaret etmektedir. Ayrıca, akciğerler ve akciğeri drene eden lenf nodları toplandı ve işlenerek dokuyu infiltre eden bağışıklık hücrelerini izole etmek için ayrıntılı immünofenotipleme gerçekleştirildi ve farklı tedavi grupları arasında immün hücre popülasyonlarındaki farklar karşılaştırıldı. Kontrol grubu (NNK + salin) ile karşılaştırıldığında, SA-4-1BBL'nin akciğerlerde ve akciğeri drene eden lenf nodlarında CD4+ merkezi bellek T hücrelerinin (CD4+CD44yüksekCD62Lyüksek) mutlak hücre sayısını önemli ölçüde artırdığı gösterildi ($p < 0.05$). SA-4-1BBL tedavi grubunun akciğeri drene eden lenf nodlarında, naif CD4+ T lenfositlerinin (CD4+CD44düşükCD62Lyüksek) sayısı kontrol grubuna göre önemli ölçüde daha yüksekti. Dahası, SA-4-1BBL tedavisi alan hayvanların akciğeri drene eden lenf nodlarında, SA-4-1BBL'nin immünomodülatör etkisi ile, PD-1+ CD8+ T lenfositlerinin

mutlak hücre sayısında önemli bir azalma gözlemlendi. Programlanmış hücre ölüm protein 1 (PD-1) reseptörü, öncelikle aktive T hücrelerinin hücre membranlarında ifade edilen kritik bir immün kontrol noktası reseptörüdür. PD-1/PD-L1 bağlanması, immün aktivasyonu azaltan inhibe edici sinyaller sağlar. SA-4-1BBL tedavisi alan grupta PD-1+ CD8+ T lenfositlerindeki azalma, antitümöral immün modülatör etkisini desteklemek için ek bir mekanizma olarak hizmet edebilir. Çalışma sonuçlarımızda, SA-4-1BBL tedavisiyle akciğer kanseri gelişiminin baskılanmış olduğu gözlemlendi. Bu baskılanmada, T lenfositler ve NK (doğal öldürücü) hücrelerin önemli rol oynadığı bulundu. Bu immün hücrelerin in vivo baskılanmasının da SA-4-1BBL'nin antitümöral koruyucu etkisinin azalmasında sorumlu olduğu gösterildi. Tez çalışması sonuçlarımız, immün kontrol noktası uyarıcısı olan SA-4-1BBL'nin kimyasal olarak oluşturulmuş prelinik akciğer kanseri modelinde tek ajan olarak koruyucu immün yanıt oluşturacak bir aday olduğunu göstermektedir.

Anahtar kelimeler: 4-1BB, kanser immünoterapisi, akciğer kanseri, NNK,
immünomodulasyon

Destekleyen kurum: Bu tez projesi, ABD Savunma Bakanlığı tarafından desteklenmiştir.

TABLE OF CONTENTS

CONFIRMATION PAGE	iii
YAYIMLAMA VE FİKRİ MÜLKİYET HAKLARI BEYANI	iv
ETHICS STATEMENT PAGE	v
ACKNOWLEDGEMENTS	vi
ABSTRACT	vii
ÖZET	xi
TABLE OF CONTENTS	xiv
SYMBOLS AND ABBREVIATIONS	xvi
FIGURES	xvii
TABLES	xviii
1. INTRODUCTION	1
2. GENERAL INFORMATION	2
2.1 Information about cancer and epidemiology	
2.1.1. Risk factors and etiologies of cancer	
2.1.2. Epidemiology of Cancer	
2.1.3. Current Success Rates of Cancer Therapy	
2.2 Information about lung cancer, smoking, and NNK	
2.2.1. Lung cancer	
2.2.2. Epidemiology of Smoking and Lung Cancer	
2.2.3. Biological mechanisms underlying smoking-induced lung cancer	
2.2.4. The Most Potent Carcinogen Form of Nicotine: NNK (4-(methylnitrosamino)-1-(3-pyridyl)-1-butanone)	
2.3 A/J mice and lung tumor models	
2.4 T lymphocytes	
2.4.1. T Lymphocytes: The Architectures of Adaptive Immunity	
2.4.2. T Lymphocytes in Cancer: Guardians and Adversaries	
2.4.3. T cell activation, costimulation, CD137	
2.5 Exploring CD137 as an Immunotherapeutic Beacon	
2.6 SA-4-1BBL in Cancer Therapy	
3 MATERIALS AND METHODS	13
3.1 Animals	
3.2 Administration of NNK	
3.3 Construction and Expression of Chimeric 4-1BB Ligand (SA-4-1BBL)	
3.4 SA-4-1BBL Protein Administration	
3.5 Sacrifice/ Dissection	
3.6 Lung Perfusion and Sample Preparation	
3.7 Macroscopic Tumor Nodule Evaluation	
3.8 Lung Sample Preparation and Sectioning	

3.9	Histopathological Assessment of the Lungs for Microscopic Tumor Nodule Formation	
3.10	Microscopic Tumor Nodules Area Analysis	
3.11	Immunofluorescence Staining	
3.12	Confocal Microscopy	
3.13	<i>In vivo</i> Immune Cell Depletion	
3.14	Peripheral Blood Processing and Staining for Flow Cytometric Analysis of <i>in vivo</i> Depletion.	
3.15	Lung and Lung Draining Lymph Nodes Processing and Staining for Flow Cytometry and Immunophenotyping.	
3.16	Flow Cytometry	
3.17	Statistical Analyses	
4	FINDINGS	33
4.1	NNK Administration- Induced Lung Tumorigenesis in A/J Mice	
4.2	SA-4-1BBL Treatment Significantly Limited the Tumor Nodule Formation in Long-Term NNK- Exposed A/J Mice Model.	
4.3	CD4, CD8 T Cells and NK Cells Were Essential Players for SA-4-1BBL Mediated Prevention Against NNK- Induced Lung Cancer.	
4.4	Treatment with SA-4-1BBL Monotherapy Boosted Central Memory CD4+ T Cells and Naïve CD4+ T Cells and Reduced the Formation of PD-1+ CD8 T Cells.	
5	DISCUSSION	48
6	RESULTS AND SUGGESTIONS	52
7	REFERENCES	53
8	APPENDIX -1	61
	APPENDIX -2	62
	APPENDIX -3	63
9	CURRICULUM VITAE	64

SYMBOLS AND ABBREVIATIONS

ALK – Anaplastic lymphoma kinase
ANOVA – Analysis of variance
APC – Antigen presenting cells
BiTE - Bi-specific T-cell engager
CAR – Chimeric antigen receptors
CD – Cluster of differentiation
CTLA-4 - Cytotoxic T lymphocyte antigen-4
DMBA/TPA - 2,4-dimetoksibenzaldehit/ 12-O-tetradecanoylphorbol 13-asetat
DMEM - Dulbecco's Modified Eagle Medium
DMSO - Dimethyl sulfide
EGFR - Epidermal growth factor receptor
FOXP3 - Forkhead box protein P3
FSC – Forward scatter
H&E - Hematoxylin and eosin
i.p. - Intraperitoneal injection
IFN γ - Interferon γ
IHC - Immunohistochemical staining
IL - Interleukin
irAE – Immune related adverse effects
KRAS – Kristen rat sarcoma
MCA - 3-Metilkolantrane
NSCLC – Non- small cell lung cancer
NK – Natural killer
NNK - 4-(Methylnitrosamino)-1-(3-pyridyl)-1-butanone
PAH – Polycyclic aromatic hydrocarbons
PCNA - Proliferating cell nuclear antigen
PD-1 - Programmed cell death protein-1
PD-L1 - Programmed death-ligand 1
RB1 - Retinoblastoma
s.c. - Subcutaneous injection
SA – Streptavidin
SCC – Squamous cell cancer
SCLC – Small cell lung cancer
SSC – Side scatter
Th – T helper cells
TNF – Tumor necrosis factor
Treg – Regulatory T cells
TSN – Tobacco specific nitrosamines
VOC – Volatile organic compounds

FIGURES

Figure	Pages
1. Tobacco-specific nitrosamines form by nicotine nitrosation.	6
2. CD137 (4-1BB) expression and interactions in various immune cell populations.	11
3. Roles and effects of CD137 (4-1BB) receptor signal on T cell populations and other immune cell populations.	11
4. Figure 4a (left), abdominal and thoracic organs are visible after dissection, and in Figure 4b (right), lymph nodes.	21
5. The main gating strategy to classify cell populations in FCS Express software.	31
6. Treatment scheme of A/J mice to evaluate the carcinogenic effects of NNK and immunomodulatory effects of SA-4-1BBL.	33
7. Body weights of the animals during the 18-week follow-up.	34
8. Macroscopic tumor nodules (Figure 8a, left), and macroscopic tumor nodules numbers in SA-4-1BBL treated and non-treated groups (Figure 8b, right).	35
9. PCNA staining in SA-4-1BBL treated and non-treated lungs.	36
10. Microscopic tumor nodule numbers in SA-4-1BBL treated and non-treated groups.	37
11. Digital microscopy images of hematoxylin and eosin stained lung sections.	37
12. Tumor area measurement of microscopic tumor nodules from each lung section.	38
13. Percentages of microscopic tumor nodule areas to total lung areas between different treatment groups.	38
14. Experimental design of SA-4-1BBL treated and non-treated A/J mice with or without <i>in vivo</i> antibody administration.	39
15. Body weights of the animals with or without SA-4-1BBL and <i>in vivo</i> cell depletion during the 18-week follow-up.	40
16. CD4+ and CD8+ T lymphocyte populations in non-depleted and <i>in vivo</i> depletion antibodies administered groups' peripheral blood, lung, and lung draining lymph node samples at 72 hours and 12 weeks post depletion.	40, 41
17. Macroscopic tumor nodules (black circles) in different groups with or without SA-4-1BBL therapy and <i>in vivo</i> immune cell depletion.	42
18. Macroscopic tumor nodule numbers in different groups with or without SA-4-1BBL therapy and <i>in vivo</i> immune cell depletion.	42
19. Microscopic tumor nodule numbers in different groups with or without SA-4-1BBL therapy and <i>in vivo</i> immune cell depletion.	42
20. The mass dissected from the chin of an animal from the CD4+ cells depleted group (Figure 20a), hematoxylin and eosin staining (Figure 20b), and PCNA staining of the same tissue (Figure 20c).	43
21. Immunophenotyping of the mass dissected from the chin of one <i>in vivo</i> CD4+ cell depleted animal. PD1+ CD4+ cells (Figure 21a, left) and PD1+ CD8+ cells (Figure 21b, right) compared with the lung tissues from the same animal.	44
22. Digital microscopy images of hematoxylin and eosin stained lung sections in <i>in vivo</i> cell depletion groups.	45
23. CD4+ central memory T cells (CD4+CD44hiCD62Lhi) in lungs (Figure 23a), and lung draining lymph nodes (Figure 23b), naïve CD4+ T lymphocytes (CD4+CD44loCD62Lhi) in (Figure 23c), and PD1+ CD8+ cells (Figure 23d) in lung draining lymph nodes of the animals with or without SA-4-1BBL and <i>in vivo</i> cell depletions.	46

TABLES

Table	Pages
1. A comprehensive list of the experimental groups.	13
2. A comprehensive list of the tools and devices.	15
3. A comprehensive list of the chemical reagents, kits, and buffer solutions.	17
4. A comprehensive list of the antibodies used in immunofluorescence staining of lung tissues.	24
5. A comprehensive list of the antibodies for <i>in vivo</i> depletion	25
6. A comprehensive list of the flow cytometry antibodies in peripheral blood immunophenotyping.	26
7. A comprehensive list of the flow cytometry antibodies used in this thesis for lung and draining lymph node immunophenotyping.	27
8. A comprehensive list of the flow cytometry antibodies used in the lung and draining lymph node immunophenotyping for determining lymphoid/ myeloid cell populations.	30

1. INTRODUCTION

In recent years, immunotherapeutic approaches based on checkpoint inhibitors have shown remarkable progress and high success rates for treating malignancies. The immune co-stimulation pathway is a promising target to augment antitumoral immune responses by overcoming the immunosuppressive tumor niche, which can lead to resistance to therapies with immune checkpoint inhibitors. CD137, also called 4-1BB, can be used for effective immune costimulation. The 4-1BB/ 4-1BBL binding initiates a potent costimulatory response essential in effective T lymphocyte proliferation, function, and longer timespans. One limitation of using 4-1BBL is that it has a costimulatory function in its soluble form. To overcome this obstacle, a recombinant form of the 4-1BB ligand was produced by integrating the extracellular portions of murine 4-1BB ligand into a modified variant of streptavidin (SA-4-1BBL). In this thesis study, we aimed to prevent lung tumor formation in a preclinical model by using a nicotine derivative, NNK, and see the immunomodulatory effects. To induce lung tumorigenesis in A/J mice, for eight weeks, tobacco carcinogen NNK was intraperitoneally applied. To investigate the effects of SA-4-1BBL treatment, mice were subcutaneously injected simultaneously with SA-4-1BBL. We showed that lung tumorigenesis was inhibited in animals by SA-4-1BBL treatment. T lymphocytes and NK cells were essential for this inhibition; thus, *in vivo* depletion of these immune cells weakened the antitumoral protective effect of SA-4-1BBL. The SA-4-1BBL administration significantly decreased microscopic and macroscopic lung tumor nodule formation during eight weeks of exposition to NNK. This study suggests that the SA-4-1BBL agent can be a single treatment candidate to develop a protective antitumoral immune response for NNK-induced lung tumorigenesis in mice. To our knowledge, this is one of the first studies to show that immune checkpoint stimulators can be used to prevent chemically induced lung cancer. These results may be extended to different scenarios in other malignancies, including breast and prostate cancers. By their nature, with improved diagnostics, they can be detected at the preneoplastic stage, and their carcinogenesis can be stopped in the early stages using potent molecules, such as SA-4-1BBL.

2. GENERAL INFORMATION

2.1 Information about cancer and epidemiology

2.1.1 Risk factors and etiologies of cancer

Cancer has a multifactorial and complex nature that is triggered and progressed by a combination of lifestyle, environmental, and genetic determinants (1). Approximately one-third of cancer-related deaths result from modifiable risk factors and can be reduced by 30%–50% by avoiding these factors and using screening and early detection methods. Known major risk factors for cancer formation include tobacco exposure, alcohol intake, obesity, exposure to ultraviolet radiation, infectious agents (e.g., human papillomavirus, *Helicobacter pylori*), and genetic predisposition (2,3). Environmental exposure to carcinogens, such as asbestos, benzene, and radon gas can also increase the risk of cancer (4). Furthermore, diet styles, such as high levels of processed meat consumption, insufficient intake of fruits and vegetables, and consumption of preserved or canned foods containing nitrates, may contribute to cancer development (5).

2.1.2 Epidemiology of Cancer

Cancer is one of the major public health concerns worldwide, with each year millions of newly diagnosed cases. As reported by the World Health Organization (WHO), cancer is the second leading etiology of mortality globally, back of cardiovascular diseases. Cancer is responsible for an approximated 10 million deaths only in 2020. The prevalence of common cancer types varies globally; however, breast, lung, and colorectal cancers are the most frequently diagnosed cancer types globally in 2020. Breast cancer accounts for approximately 2.26 million newly diagnosed patients, followed closely by lung cancer with 2.21 million new patients, and colorectal cancer with 1.93 million new patients. Despite not being the most prevalent as measured new cases, lung cancer was associated with the highest mortality rate in 2020, resulting in approximately 1.8 million deaths (6). In the United States, cancer remains a major reason of morbidity and mortality, with approximately 1.9 million new cancer cases and 609,000 cancer-related deaths projected in 2022 (7). Cancer mortality rates depend on cancer type, with lung cancer being the principal cause of cancer-related mortality worldwide (8).

2.1.3 Current Success Rates of Cancer Therapies

The success of cancer therapy depends on various factors, including cancer type, stage at diagnosis, current treatment modalities, and patient-specific factors (age, comorbidities, and sex). Some cancers, such as certain subtypes of skin cancer, like basal cell carcinoma and early-stage breast cancer, have high cure rates with appropriate treatment (9). The therapy success rates for advanced or metastatic cancers are mostly not as high as those for other cancer types, and many patients may require further treatment or may be selected for palliative care to manage symptoms and improve their quality of life (10). Thus, despite advances in early detection methods and promising treatment approaches, cancer mortality rates remain high, highlighting the need for cancer research and improving therapeutic strategies in the future (11).

2.2 Information about smoking, cigarette smoke and NNK

2.2.1 Lung cancer

2.2.1.1 Histological Diversity

Lung malignancies are classified into diverse histopathological classes, with non-small cell (NSCLC) and small cell lung cancer (SCLC) representing the major categories. NSCLC includes the histopathological classes as adenocarcinoma, squamous cell carcinoma (SCC), and large cell carcinoma, covering approximately 85% of all lung malignancies diagnosed in the clinic, each exhibiting distinct clinicopathological features and therapeutic implications (12). SCLC, although less prevalent among patients diagnosed with lung cancer, has unique challenges owing to its aggressive nature and limited treatment options (13).

2.2.1.2 Molecular Landscape

Advances in molecular oncology have resolved the genomic landscape of lung cancer by uncovering distinct driver mutations and molecular alterations. Mutations in genes such as EGFR, ALK, ROS1, and BRAF in NSCLC and molecular alterations in TP53 and RB1 in SCLC have become essential in guiding targeted therapies and determining the prognosis (14).

2.2.1.3 Challenges in Early Detection and Diagnosis

Early detection remains a formidable challenge in lung cancer management, with a substantial number of cases being diagnosed at advanced stages. This delayed diagnosis complicates treatment strategies and contributes to the overall high

mortality rate of the disease (15). Clinical management of lung cancer remains a formidable challenge, compounded by late-stage presentations and intrinsic resistance to conventional treatments. Despite these challenges, the last decade has witnessed significant strides in therapeutic paradigms, including the advent of immune checkpoint inhibitors and targeted therapies that have ushered in a new era of precision medicine (16). Therapeutically, lung cancer management has undergone transformative shifts with the advent of targeted therapies and immune checkpoint inhibitors. However, challenges such as intrinsic and acquired resistance to treatment, coupled with the elusive nature of certain subtypes, such as SCLC, underscore the need for continued research and innovation (17).

2.2.1.4 Approved and Promising Immune-Based Therapies in Lung Cancer: A Clinical Revolution

Over the past three decades, a multitude of therapeutic strategies have been employed for Small Cell Lung Cancer (SCLC); nevertheless, there remains a notable absence of groundbreaking advancements that could enhance the overall survival rates (18). While the impact of the immune system on cancer has been recognized for an extended period, recent research has led to the approval of immunotherapeutic approaches, such as immune checkpoint inhibitors, oncolytic viruses, and BiTE antibody constructs, for clinical use (19). CAR-T cell therapies, exemplified by axicabtagene ciloleucel (Yescarta) and tisagenlecleucel (Kymriah), have shown the potential of engineered T cells to target hematological malignancies (20). Bispecific antibodies such as blinatumomab have highlighted innovative approaches that directly redirect immune cells to engage cancer cells (21). In addition, the emergence of immune checkpoint inhibitors, like anti-PD1 (nivolumab) and anti-CTLA-4 (ipilimumab), has marked a watershed moment in cancer treatment. Since 2015, they have been administered in clinical settings for non-small cell and small cell lung cancer since 2018. These immune therapies, by releasing the brake mechanisms of T cell activation, have induced significant efficacy across various types of malignancies, from melanoma to lung cancer. The clinical success rate of these agents has been indicated in clinical trials, including the CheckMate and KEYNOTE studies, validating the efficacy and safety profiles (22–24). Despite using combination therapies, the overall response rate (ORR) was 25%. Additionally, the administration of immune checkpoint inhibitors continues to be plagued by the frequent occurrence of immune-related adverse effects (irAEs), compounding the challenge of low therapeutic efficacy (25). This underscores the crucial role of immune system modulation as a pivotal element in generating a response against lung cancer, particularly in the context of smoking. Consequently, there is a need to develop innovative immune intervention strategies that utilize novel therapeutic molecules

in a preventive orientation. Modulating immune responses holds the potential to specifically target high-risk populations, including individuals with a history of smoking or passive smokers who are susceptible to Small Cell Lung Cancer characterized by a complex tumor mutational burden (25).

2.2.2. Epidemiology of Smoking and Lung Cancer

Smoking is the leading etiology of lung cancer pathogenesis, with approximately 85% of cases attributed to tobacco smoke exposure. According to World Health Organization (WHO) data, tobacco use, and exposure are responsible for more than 7 million mortality per year globally, with over 6 million deaths attributed to direct tobacco use and approximately 890,000 deaths due to secondhand smoke exposure (15). In the United States, lung cancer is the second most common malignancy and the main cancer type of cancer-related death in both sexes (26).

2.2.3. Biological mechanisms underlying smoking-induced lung cancer.

Tobacco smoke contains more than 7000 toxic chemicals, including tobacco-specific nitrosamines (TSNAs), polycyclic aromatic hydrocarbons (PAHs), volatile organic compounds (VOCs), and aromatic amines. (27). These carcinogens can induce DNA damage, cause mutations, and genomic instability in lung cells, which can drive the induction and advancement of lung cancer (28). Furthermore, it can promote inflammation, oxidative stress, and immune dysregulation in the lung microenvironment, which can contribute to carcinogenesis, allergies, asthma, and other lung diseases (29).

2.2.4. The Most Potent Carcinogen Form of Nicotine: NNK (4-(methylnitrosamino)-1-(3-pyridyl)-1-butanone)

In tobacco, the main alkaloid found is nicotine, but by nitrosation tobacco-specific nitrosamines occur (Figure 1) (27) . Despite the incomplete understanding of the carcinogenic mechanisms of nicotine, 4-(methylnitrosamino)-1-(3-pyridyl)-1-butanone (NNK) remains as the most potent carcinogenic nitrosamine form of nicotine in both humans and various classes of animals (30–32).

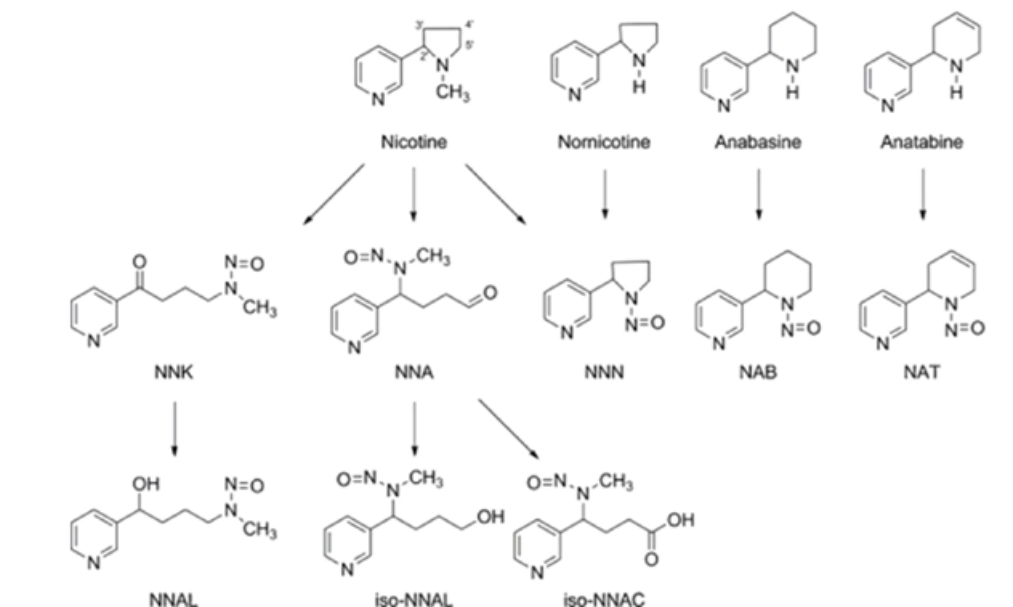


Figure 1. Tobacco-specific nitrosamines form by nicotine nitrosation. (27)

2.3. A/J mice and lung tumor models

Mouse models are invaluable tools to unravel the complexities of various diseases in preclinical research. In cancer research, specific models are used to explore tumorigenesis, progression, and therapeutic interventions. Mouse models are at the forefront of preclinical research and offer insights into the intricacies of lung cancer that transcend the limitations of *in vitro* studies. These models, with their genetic, physiological, and immunological similarities to humans, provide a platform for understanding the molecular mechanisms, genetic predispositions, and environmental influences that contribute to lung cancer development (33). Different mouse strains utilized in lung cancer research exhibit heterogeneity among human populations. Each mouse strain harbors unique genetic backgrounds, different levels of susceptibility to carcinogens, and responses to therapeutic interventions, allowing cancer researchers to adapt their investigations to specific aspects of lung cancer biology (34). Among the different mouse strains, A/J mice have emerged as a particularly valuable model for studying smoking-related lung cancer. This strain exhibits increased susceptibility to lung adenocarcinoma upon exposure to tobacco smoke and its derivatives, making it an applicable model for replicating the human scenario of smoking-associated lung cancer (35,36). A/J mice, characterized by their genetic predisposition and increased sensitivity to lung carcinogens, have been extensively employed in preclinical studies exploring the etiology and progression of lung cancer (30–32,37,38). Notably, the Ah locus, responsible for the metabolism of polycyclic aromatic hydrocarbons found in tobacco smoke (39), and the Pas1 locus

related to the Kras2 gene play a critical role in the strain's heightened vulnerability to smoking-related lung cancer (40).

2.4. T lymphocytes

2.4.1. T Lymphocytes: The Architectures of Adaptive Immunity

T lymphocytes, which are generated in the bone marrow and “educated” in the thymus, represent a diverse population of immune cells with specialized functions against infections and malignancies. CD8⁺ (cytotoxic) T cells and CD4⁺ (helper) T cells form the essence of T-cell diversity, each of which has distinct roles in immune surveillance and response (41). The T cell activation hinges on the intricate interplay of T cell receptors with antigen-presenting cells (APC), guiding the immune cells toward a specialized defense against specific threats such as infections and malignancies. Through antigen presentation and activation, T cell metabolism changes to adapt to the differentiation of distinct T cell subtypes (42).

2.4.2. T Lymphocytes in Cancer: Guardians and Adversaries

Within the complexity of cancer biology and immunology, T lymphocytes have emerged as pivotal players with dual roles in malignancies. Immune surveillance, the potential of T lymphocytes to identify and eliminate aberrant cells, is a critical defense mechanism against tumorigenesis (43). Nevertheless, cancer cells often develop various immune evasion strategies, creating an immunosuppressive tumor microenvironment that compromises effective T cell function and even modifies their metabolism (44). This elaborate interplay highlights the importance of understanding the biology of T-cell subtypes in the context of cancer. T cells are classified into subtypes depending on their immune function using specific cell markers.

2.4.2.1. CD8⁺ (Cytotoxic) T Cells

CD8⁺ (cytotoxic) T cells are the main T cell population that play a role in antitumor immune defense. With their T-cell receptors, they recognize tumor antigens present on aberrant cancer cells with their MHC-I. Subsequently, they employed perforin-and granzyme-B-mediated cytotoxicity. After finishing their effector functions, some cells exhibited effector and central memory (T_{cm} and T_{em}).

2.4.2.2. Central Memory T Cells (T_{cm})

They are a subset of memory CD8⁺ (cytotoxic) T cells that contribute to long-term immune memory after the eradication of infections or malignancies (45). They were identified by their CCR7, CD45RO, and CD62L antigens. Likewise, they are mostly found in secondary (peripheral) lymphoid organs (spleen and lymph nodes), and CD62L plays a role in their entry into lymph nodes through the high endothelial venules (46). In addition, they patrol between the blood and secondary (peripheral) lymphoid organs. Owing to their homing features to lymphoid tissues, they play a role in rapid responses upon re-exposure to antigens specific to them. After antigen recognition, they exhibited a higher proliferative response than naive T cells. T-bet and Eomes play important roles in transcriptional regulation (47). Bcl-6 expression induces a stem cell-like phenotype. Their lifespan is longer than that of the effector memory (T_{em}) and effector T cells.

2.4.2.3. Effector Memory T cells (T_{em})

Unlike T_{cm}, its primary role is to supply quick responses in peripheral tissues. Their lifespan was shorter than that of the T_{cm} cells. They express CD45RO but do not express CCR7 and can be differentiated from T_{cm} cells using this marker. They can be found in non-lymphoid tissues as first defenders, especially for local infections. Their transcriptional regulation is dominated by T-bet to prime immediate effector functions (47).

2.4.2.4. Helper T Cells (CD4⁺ T Cells)

They contribute to fine-tuned immune responses through their subsets. CD4⁺ T cells are subclassified into subsets based on their immune function using cell markers (48–50).

2.4.2.5. Th1 Cells (T-helper 1)

They secrete TNF- α and IFN- γ to promote cell-mediated cytotoxic responses against pathogens and aberrant cells, such as cancer cells (49,50).

2.4.2.6. Th2 Cells (T-helper 2)

They can be identified by their IL-4, IL-5, and IL-13 secretion properties. They conduct humoral immunity and take a role in B cell activation and maturation.

Furthermore, they may contribute to an immunosuppressive microenvironment in tumorigenesis (49,50).

2.4.2.7. Th17 Cells (T-helper 17)

Their IL-17, IL-21, and IL-22 secretion differentiates them from other CD4+ T cell subtypes. They involve inflammatory responses in mucosal surfaces (49,51,52).

2.4.2.8. Regulatory T Cells (Treg)

Their main role is tailoring local immune responses by providing suppression mechanisms. They secrete IL-10, and TGF- β inhibitory cytokines to regulate immune response in the environment. They express CD4, CD25, and Foxp3 and can be detected by these markers (53).

2.4.2.9. Gamma Delta T Cells ($\gamma\delta$ T Cells)

Differently from CD4 and CD8 T cells, gamma delta T cells express a T cell receptor constructed with γ and δ subunits and distinguished by this molecule. This feature gives them the capacity to recognize unconventional antigens, especially stress-induced molecules, and non-peptide antigens. In cancer, they play a role in tumor immunosurveillance. They are located especially at mucosal sites involved in immune surveillance (54).

2.4.3. T cell activation, costimulation, CD137

The activation of naive T cells involves three pivotal stages according to the current understanding (55). The first stage, known as "Signal-1", encompasses the binding between the T cell receptor and the peptide antigen containing major histocompatibility complex (MHC) (56). Moving on to "Signal-2", this stage results from the interaction of costimulatory molecules with their receptors, which can be either stimulator (activator) molecules, like CD28/B7-1, or inhibitory, as seen in CTLA-4/CD80 interactions (57). These costimulatory molecules play a critical role in governing T cell regulation and maintaining the balance of immune responses (55). After costimulation, "Signal-3" comes into play, inducing the differentiation and expansion of T cells driven by cytokines. The precise sequence of these three steps is of utmost importance, and any pre-exposure can potentially inhibit the activation of T cells (58).

2.5. Exploring CD137 as an Immunotherapeutic Beacon

Between the options of potential immunotherapeutic targets, CD137 (4-1BB) emerges as a signal of promise. CD137, also known as 4-1BB, is a co-stimulator molecule belonging to the tumor necrosis factor receptor (TNFR) superfamily and can be named as TNFR-9 (59). The CD137 receptor is not continuously expressed on immune cells but it can be found in various immune cell populations (Figure 2) (59). The expression starts with the immune activation of the cells. As illustrated in Figure 3, activation of CD137 enhances the proliferation and survival capacities of T cells (60), the cytotoxic activity of NK cells (61,62), mature B lymphocyte formation (63) and dendritic cells (64,65), rendering them attractive candidates for clinical translation. CD137 plays an essential role in regulating immune responses by providing co-stimulatory signals to T lymphocytes by binding with its ligand, CD137L (4-1BBL) (66). Following the cloning of the natural ligand for CD137, known as CD137L (4-1BBL), preclinical studies in mice demonstrated that administering 4-1BBL yielded therapeutic benefits in diverse solid tumors (67) and hematological malignancies (68). Preclinical studies involving CD137 agonists, like urelumab and utomilumab, have enlightened their potential to boost antitumoral immune responses (69–71). CD137 agonists can also promote the memory T cell differentiation, providing long-lasting immune memory against tumor antigens (69,70). While agonistic 4-1BB antibodies have been utilized in both preclinical studies (72) and clinical trials (73), their application has been hindered by reported complications, notably hepatotoxicity. This limitation poses challenges for the broader adoption of approaches involving agonistic 4-1BB monoclonal antibodies.

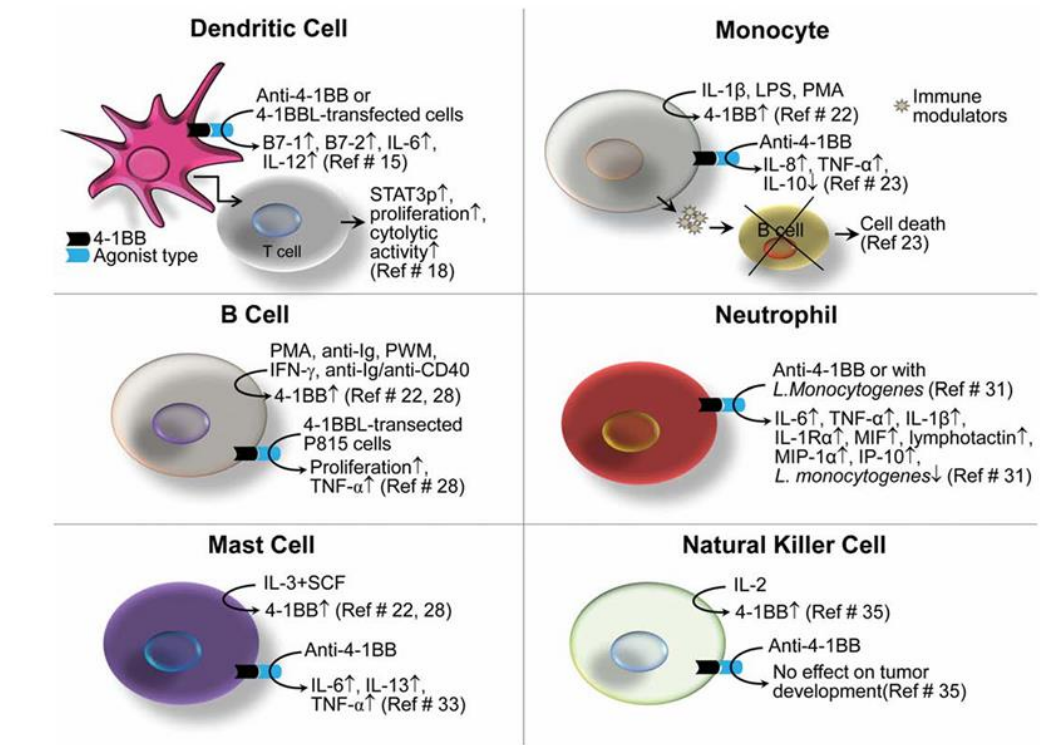


Figure 2. CD137 (4-1BB) expression and interactions in various immune cell populations (59).

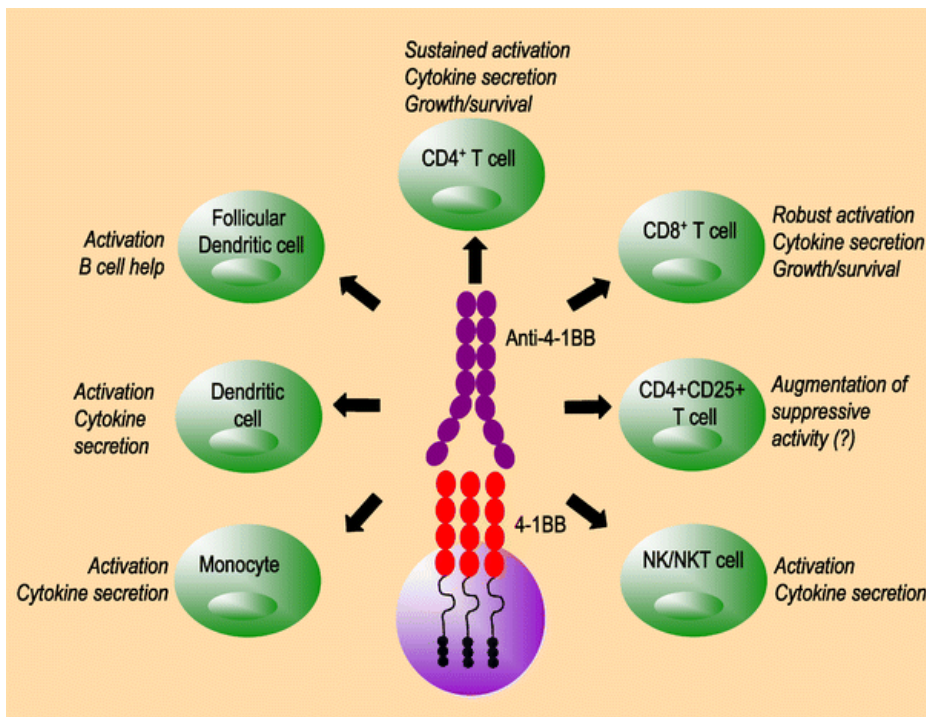


Figure 3. Roles and effects of CD137 (4-1BB) receptor signal on T cell populations and other immune cell populations. (60)

2.6. SA-4-1BBL in Cancer Therapy

SA-4-1BBL is a novel immunomodulatory molecule designed to enhance the immune response against cancer cells (61). It is a chimeric protein structure, made from extracellular domains of mouse 4-1BBL molecule and streptavidin (74). The functional form of the SA-4-1BBL molecule necessitates the assembly of soluble tetramers and oligomers *in vivo*. Studies have indicated that SA-4-1BBL inhibits the generation of regulatory T cells (CD4+CD25+FOXP3+) by inducing IFN- γ synthesis in conventional T cells (62). SA-4-1BBL activates the 4-1BB pathway, providing potent co-stimulatory signals to promote T lymphocyte activation and natural killer cells (75). SA-4-1BBL has been pointed out to inhibit tumor growth and boost survival in animal models. Furthermore, the administration of SA-4-1BBL exhibited immunoprotective effects without inducing complications such as systemic cytokine storm or hepatitis (75).

In this research project, we have shown that the potential for usage in immunotherapy of novel SA-4-1BBL molecule is not limited to previously used preclinical cell-line derived subcutaneous tumor models. Also, it includes carcinogen (NNK) -induced lung cancer in preclinical mouse strains with high susceptibility to tobacco carcinogen-induced tumors. This thesis study reveals that SA-4-1BBL as a single therapeutic molecule evokes a protective and effective antitumoral immune response against lung cancer formation under smoke-related carcinogen exposure. Future studies of the mechanisms governing immune checkpoint stimulation may contribute to further therapeutic approaches to combine this molecule with other biologics for enhanced immunological efficacy. Above all, a therapy that includes this immunotherapeutic molecule can be adapted to use in numerous cancer types, such as breast and prostate cancer, cancer types can be diagnosed in early stages, even in preneoplastic stages.

3. MATERIALS AND METHODS

3.1 Animals

NNK susceptible A/J mice (18–22 g, female) were purchased from The Jackson Laboratory (Stock #000646; Bar Harbor, ME, JAX) and kept in the University of Missouri - Columbia animal facility. A/J mice were housed in plastic ventilated cages with ad libitum food and water access, under strictly regulated conditions of 22 °C and 45% relative humidity, and a 12-h light-dark day cycle. The cages of mice were cleaned weekly by animal facility personnel, and mice were monitored weekly during experimental periods. The mice were randomly separated into groups, as shown in the experimental groups' list. A comprehensive list of experimental groups can be found in Table 1. Each animal's ear was tagged at the beginning of the experiment, to follow up on their clinical status and body weights each week of the follow-up. Ethics approval of the thesis study protocol was conducted by the Animal Care and Use Committee of the University of Missouri-Columbia, with a protocol number IACUC–9893. It can be found in the Appendix section.

A comprehensive list of the experimental groups in this study is presented in Table 1.

Table 1 **Experimental groups**

GROUP NAME	GROUP INFORMATION
NAÏVE A/J	NO NNK, NO SA-4-1BBL ADMINISTRATION, NO DEPLETION
NNK+VEHICLE	NNK (+), NO SA-4-1BBL ADMINISTRATION, NO DEPLETION
NNK+SA-4-1BBL	NNK (+), SA-4-1BBL (+), NO DEPLETION
NNK+SA-4-1BBL, CD4 DEPLETED	NNK (+), SA-4-1BBL (+), CD4 T CELL DEPLETION
NNK+SA-4-1BBL, CD8 DEPLETED	NNK (+), SA-4-1BBL (+), CD8 T CELL DEPLETION
NNK+SA-4-1BBL, NK DEPLETED	NNK (+), SA-4-1BBL (+), NK CELL DEPLETION

3.2 Administration of NNK

The carcinogen NNK (4-(Methylnitrosamino)-1-(3-pyridyl)-1-butanone) was purchased from Santa Cruz Biotechnology (Cat#: sc-209854) and later dissolved in DMSO (dimethyl sulfide; Sigma, Cat#: D2650) to be stored as 50 mg/ml stock solution in -20°C. On the day of injections, 25 mg/kg doses of NNK were made using sterile PBS (Gibco, Cat#: 10010-023) as a solvent, and intraperitoneally injected using a BD 1 ml insulin syringe (BD Company, Cat#: 329622) and 18G x 1 1/2 needle (BD Company, Cat#: 2088564) for each week of eight following weeks. The naive (control) group was injected with vehicle, sterile saline. Tools and devices (Table 2), chemical reagents, kits, and buffer solutions (Table 3) used for the thesis study mentioned through materials and methods can be found in Table 2 and Table 3.

A comprehensive list of the tools and devices used in this thesis study is presented in Table 2.

Table 2 **Tools and devices**

PRODUCT NAME	COMPANY NAME AND COUNTRY
Hemocytometer	Marienfeld, Germany
Fisher Vortex Genie 2	Fisher Scientific, USA
Ice maker	Hoshizaki, Japan
-80°C refrigerator	
-20°C refrigerator, TSX Series	Thermo Scientific, USA
4°C refrigerator	Thermo Scientific, USA
Trans-Blot membrane transfer system	Bio-Rad, USA
Electrophoresis power source	Bio-Rad, USA
Gel running tank	Bio-Rad, USA
CO ₂ tank	
Invitrogen EVOS M7000 Imaging System	Thermo Fisher Scientific, USA
Invitrogen EVOS Light Cubes (DAPI, Texas Red)	Thermo Fisher Scientific, USA

Leica RM2235 Microtome	Leica, Germany
Leica HI1215 Water bath for paraffin sections	Leica, Germany
Leica TCS SP5 Confocal Microscope	Leica, Germany
Olympus CKX53 Compact Cell Culture Microscope	Olympus, Japan
OHAUS Scout® Balance Scale	OHAUS Corporation, USA
Heratherm Compact Microbiological Incubator	Thermo Scientific, USA
Fisher Scientific Isotemp 215 Dual Digital Water Bath	Fisher Scientific, USA
Mettler Toledo S20 SevenEasy pH Meter	Mettler Toledo, USA
METTLER TOLEDO ML204T/00 INTERNAL CALIBRATION ANALYTICAL BALANCE	Mettler Toledo, USA
TX-1000 4 x 1000mL Swinging Bucket Rotor	Thermo Scientific, USA
Sorvall Floor Model Centrifuge	Thermo Scientific, USA
I-24 incubator Shaker Series	New Brunswick Scientific, USA
Cytek Aurora 5 (UV16 V16 B14 YG10 R8) flow cytometer	Cytek Biosciences, USA

A comprehensive list of the chemical reagents, kits, and buffer solutions used in this thesis study is presented in Table 3.

Table 3 **Chemical reagents, kits, and buffers**

PRODUCT NAME	COMPANY NAME, CATALOG NO. AND COUNTRY
NNK (4-(Methylnitrosamino)-1-(3-pyridyl)-1-butanone)	Santa Cruz Biotechnology, Cat#: sc-209854, USA
DMSO (Dimethyl sulfide)	Sigma, Cat#: D2650, USA
PBS (Phosphate Buffered Saline)	Gibco, Cat#: 10010-023, USA
BD® 1 ml Insulin Syringe	BD Company, Cat#: 329622, USA
BD® 10 ml Syringe	BD Company, Cat#: 303134, USA
18G x 1 1/2 needle	BD Company, Cat#: 2088564, USA
Sterile cell strainer (40 µm nylon mesh)	Fisherbrand, Cat#: 22363547, USA
LPS (Lipopolysaccharide)	
PCR2.1TOPO vector	Invitrogen Life Technologies, Cat#: K450002, USA
DES (Drosophila Expression System)	Invitrogen Life Technologies, Cat#: , USA
Sepharose column	
Limulus ameocyte lysate kit	Charles River Breeding Laboratories, Cat#: ,USA
Goat anti-SA antibody (western blot)	Pierce, Cat#: 31430, USA
SA-4-1BBL	Produced in Yolcu/ Shirwan laboratory
22G needle	BD Company, Cat#: 2088564, USA
BD® 3 ml Syringe	BD Company, Cat#:309657, USA
DMEM (Dulbecco's Modified Eagle Medium) media	Gibco, Cat#: 11965-092, USA
10% Neutral Buffered Formalin	Leica Biosystems, Cat#: 3800602, Germany

Paraplast paraffin beads	Leica Biosystems, Cat#: 39601006, Germany
Fisher Tissue Path Cassettes IV Biopsy	Fisher Scientific, Cat#: 22-282255, USA
Tissue-Tek Biopsy Uni-Cassette	Sakura, Cat#: 4087, USA
Xylenes	Honeywell, Cat#: 534056, Slovakia
Eosin Y, %1 Alcoholic	Electron Microscopy Sciences, Cat#: 26051-11, USA
Mayer's hematoxylin	Electron Microscopy Sciences, Cat#: 26303-02, USA
Permount mounting medium	Fisher Chemical, Cat#: SP15-100, USA
Micro cover glass – 22mm x 50mm	Electron Microscopy Sciences, Cat#: 72200-40, USA
Premium Microscope Slides Superfrost, 3" x 1" x 1mm	Fisher Scientific, Cat#: 22-178-277, USA
MX35 Premier Plus Microtome Blade	Thermo Scientific, Cat#: 3052835, USA
Ammonium hydroxide	Sigma-Aldrich, Cat#: 221228, USA
Immu-Mount fluorescent mounting media	Epredia, Cat#: 9990402, USA
Sodium citrate buffer	Fisher Chemical, Cat#: BP3271, USA
BSA (bovine serum albumin)	Sigma, Cat#: A70300, USA
Triton-X	Sigma, Cat#: T8787, USA
Normal goat serum	ImmunoReagents Inc., Cat#: SP-004-VX2, USA
Tween-20	Sigma Aldrich, Cat#: P5927, USA
5 ml round bottom polystyrene FACS (fluorescence activated cell sorting) tubes	BD, Cat#: FSC-9005, USA
Type IV Collagenase	Worthington Biochemical, Cat#: 4186, USA
40-µm nylon cell strainer	pluriStrainer, Cat#: 43-50050-01, USA

Glass slides with frosted side	GSC International, Cat#: 1201A72, USA
100- μ m nylon mesh	Elko, Cat#: 03-100/32, USA

3.3 Construction and expression of chimeric 4-1BB ligand (SA-4-1BBL)

Splenocytes were derived from mouse spleen and stimulated with lipopolysaccharide (LPS) (5 μ g/ml) for 2 days for total RNA isolation. Isolated RNA was used for RT-PCR to amplify the extracellular portion of 4-1BBL (amino acids 104–309) using primers (sense) 5'-ATCGAATTCCGCACCGAGCCTCGGCCAGCG-3' and (antisense) 5'-GGACTCGAGCATAGCAGCTTGAGGACTTAGC-3'. The final RT-PCR product was cloned into PCR2.1TOPO vector (Invitrogen Life Technologies), and a single clone containing the precise sequence for 4-1BBL was digested using EcoRI and XhoI and subcloned into PMT/BiP/V5-HisA Drosophila expression vector containing a 6xHis Tag and core SA sequence. Chimeric 4-1BB ligand (SA-4-1BBL) was expressed using the Drosophila expression system (DES; Invitrogen Life Technologies), purified using Sepharose column, tested for endotoxins by Limulus amebocyte lysate kit (Charles River Breeding Laboratories), and quantified. The end product SA-4-1BBL protein was subjected to analysis by Western Blot under native and denaturing conditions using goat anti-SA Ab (Pierce).

3.4 SA-4-1BBL protein administration

SA-4-1BBL protein was manufactured in the laboratory, by the established protocols above, and stored at -20°C. In the six and eight weeks, 48 hours after i.p NNK injection, mice were s.c injected with 100 μ g of SA-4-1BBL, using a BD 1 ml insulin syringe (BD Company, Cat#: 329622) and 18G x 1 1/2 needle (BD Company, Cat#: 2088564), dissolved in sterile PBS (Gibco, Cat#: 10010-023). NNK control group was s.c injected with vehicle, sterile saline.

3.5 Sacrifice/ Dissection

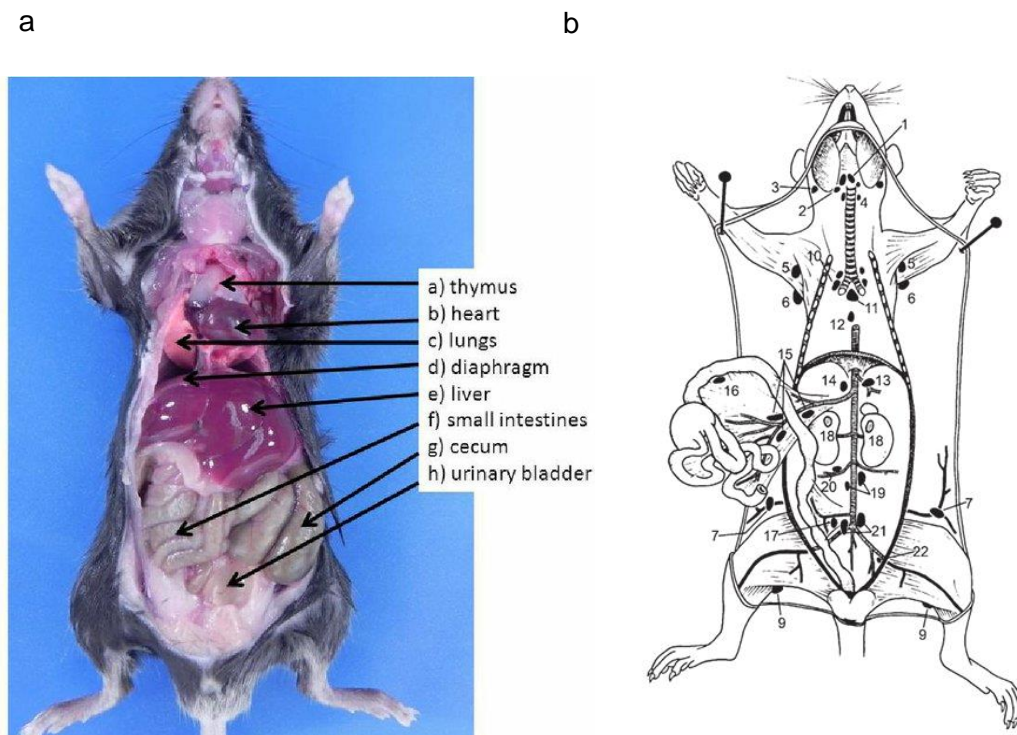
The mice were terminated at 18 weeks of the study based on the standards that were previously approved by the University of Missouri – Columbia animal ethics committee. Termination was performed using the carbon dioxide asphyxiation method (5L/ min, 2 minutes) and it was ensured by toe pinch reflex before dissection.

Following the retrieval of lungs and draining lymph nodes, mouse carcasses were disposed of in biohazard bins.

3.6 Lung perfusion and sample preparation

After termination, mice were pinned to the dissection platform from their extremities to expose all abdominal and thoracic organs by dissection as shown in Figure 4a (76). The body was opened starting with a horizontal incision from the middle of the lower abdomen using surgical scissors. From the incision, a small hole was opened, and skin and abdominal wall muscles were cut vertically, to the center of the lower part of the neck. From the lower abdominal part, lateral incisions were made to create access to the abdominal cavity and continue up to the trachea. Internal organs, such as the liver, spleen, large and small intestines, etc. were observed in the abdominal cavity for metastasis foci, and other pathologies (necrosis, fatty liver, etc.) were checked. Later, with forceps, the liver and other abdominal cavity organs were moved aside to observe the diaphragm and intra-abdominal lymph nodes (for metastasis focus) and have access to renal arteries. After exposing the diaphragm, it was evaluated for metastasis or tumor nodule formation. Later, the diaphragm was cut 1-2 mm from the right side of the investigator, and it expanded. Cut was continued from right side to left until exposing the thoracic cavity, lungs, heart, and thymus. To enable better observation and manipulation for the next steps, the rib cage was removed. Later, an incision was made to the renal artery to create a way to drain perfusion solution (1X PBS), which prevented the explosion of the heart due to increased internal volume. Next, the thymus was observed for any pathologies and gently moved to inspect the heart. For lung perfusion, a 3 mL syringe with a 22G needle was used to inject 1X PBS into the right ventricle. Lungs were perfused slowly, approximately 300–400 $\mu\text{L}/\text{second}$ with PBS to prevent tissue damage since over-inflation can lead to alveolar wall breakage and the appearance of emphysema in the histopathological analyses. With successful perfusion, the lungs' color turned light pink-white. Around 3 ml of 1X PBS was used for each mouse lung perfusion. After perfusion, the heart was lifted with forceps and separated gently from the lung. Under the heart, lung-draining lymph nodes (tracheobronchial lymph nodes were observed mostly in paratracheal zones (Shown with number 11 in Figure 4b) (77). Lymph nodes were visible with their light pink-white colors and nodular structures. From each animal, lung-draining lymph nodes were collected, and their total numbers were recorded. Dissected lung-draining lymph nodes were placed into Falcon tubes filled with DMEM media (Gibco, Cat#: 11965-092) and transferred on ice to process the tissues for immunophenotyping on the same day of termination.

Next, the lungs were dissected as a whole and put into a dish filled with 1X PBS, to observe macroscopic tumor nodules under the dissecting microscope.



Figures 4a and 4b. Figure 4a (left), abdominal and thoracic organs are visible after dissection and Figure 4b (right), lymph nodes.

3.7 Macroscopic tumor nodule evaluation

Two experienced individuals observed the entire lung with a dissecting microscope for the number of macroscopic tumor nodules with a blinded assessment of experimental groups. Macroscopic tumor nodules with a light, pink-colored feature could be observed on the lung surfaces, which made the evaluation and enumeration of the nodules easier for observers. Later, lung photographs were taken to show the macroscopic tumor nodule formation between the different experimental groups. After assessment of the lungs based on tumor presence and calculation of total macroscopic tumor nodules on each animal's lungs, lungs were separated into lobes and each lung lobes were drained using sterile sponges and weighed. Lungs were divided into pieces for histopathological analyses for microscopic tumor nodule formation, flow cytometry analyses, and other possible future experiments.

3.8 Lung sample preparation and sectioning

Later, a part of the lung tissue was put into plastic tubes labeled with each mouse ear tag number and study ID, to fix with 10% neutral-buffered formalin for use in histopathological evaluation. After keeping in formalin fixation for a minimum of 24–48 hours, samples were taken into steps for paraffin embedding. Lung tissues were placed into plastic cassettes. First, formalin was washed away from tissue with distilled water. Later, cassettes were put into ethanol and xylene washes, at room temperature for ethanol washes and 50°C oven for xylene. After xylene washes, cassettes were incubated in melted paraffin located in different containers to provide a better cover with paraffin. In the last step, tissues were taken from cassettes and put into metal trays and covered with clean paraffin, while keeping the lid of the plastic cassettes. These metal trays were kept at 4°C, overnight. The following day, solidified paraffin blocks were taken out of metal trays and stored at room temperature. Paraffin blocks were cut into sections 8 µm thick using a Leica RM2235 microtome located in the laboratory. Sections were taken on microscopic examination slides and were incubated at 4°C, overnight. Later, slides were incubated for 3 days if sections were used for immunohistochemistry. From each experimental animal's lungs, tissue sections were taken by following a standard technique to guarantee the objective evaluation. From each block, subsequent tissue sections were cut 40 µm apart. A minimum of 60 sections were taken into hematoxylin and eosin staining step for microscopic tumor nodule evaluation from each animal. All slides were stored at room temperature.

3.9 Histopathological assessment of the lungs for microscopic tumor nodule formation

Microscopic tumor formation was evaluated using the most classical histopathological technique, hematoxylin and eosin (H&E) staining. As has been already shown in the previous studies that used NNK to induce lung carcinogenesis, after 16 weeks post-NNK injection (64), immunohistopathological analysis was limited to sub-classifying lung tumors into adenoma and adenocarcinoma. Two experienced observers analyzed hematoxylin and eosin stained lung tissue sections under the Olympus CKX53 inverted microscope. To have a digitalized archive of the tissues, EVOS M7000 digital microscope and imaging system were used. With 10X optical magnification, default images were recorded from each section taken from each animal, by EVOS digital microscopy. Next, 10X, 20X, and 40X digital magnifications were used to produce final magnifications of 100X, 200X, and 400X of the sections. While evaluating, recurrent microscopic tumor nodules were accepted as one nodule. The microscopic tumor nodules were evaluated by two experienced observers to make a blinded assessment. From each animal, total microscopic tumor

nodules were calculated, and for the statistical analysis, a one-way ANOVA test was used in GraphPad Prism software, v.9.

3.10 Microscopic tumor nodules area analysis

The data of the microscopic tumor nodule areas were taken from H&E-stained lung sections. From each treatment group, five lung samples' nodule areas were analyzed. The three biggest microscopic tumor nodules were determined. An EVOS M7000 microscope (Invitrogen) was used to line the limits of the tumor nodules. The dimensions (length and width) of the microscopic tumor nodules and the total area of each lung section were measured by EVOS Analysis software. The total area of microscopic tumor nodules per lung section was calculated and shown as a percentage of total lung area. From each experimental group, a minimum of 15 lung nodules were analyzed for comparison, and statistical differences were calculated using a one-way ANOVA test in GraphPad Prism software, v.9.

3.11 Immunofluorescence staining

To mark the proliferation capacities of microscopic tumor nodules observed in H&E-stained slides, proliferating cell nuclear antigen (PCNA) antibodies were used for immunofluorescence staining. PCNA is a non-histone protein that is in the nucleus and takes a role during DNA synthesis. Thus, PCNA is one of the mainly used markers for analyzing the proliferation capacities of various neoplasms. PCNA is in use for determining the pathological grades in clinical pathology and preclinical research (65,67). Previously prepared slides mounted with paraffin sections of lung tissues were deparaffinized by washes with xylene (Fisher, Cat#: 22-143,975), rehydrated through increased concentrations of ethanol-water solutions, and washed with distilled water. The antigenic retrieval step was performed by exposing sections in 10-mM sodium citrate (Fisher Chemical, Cat#: BP3271) buffer (pH 6.0) for 15 minutes in a water bath at 100°C and washed with 1X phosphate-buffered saline (PBS). To prevent or minimize background staining, nonspecific antibody bindings were blocked by incubation with 5% bovine serum albumin (BSA, Sigma, Cat#: A70300), and 0.3% Triton-X (Sigma, Cat#: T8787) dissolved in 1X PBS. Later with a 2.5% normal goat serum (ImmunoReagents, Inc., Cat#: SP-004-VX2), and Fc block (BD Pharmingen, Cat#: 553,142, Clone: 2.4 G2) also dissolved in 1X PBS. PCNA primary antibody (Novus Bio, Cat#: NB100-456, 1:100 dilution) incubation of lung samples were done overnight at 4 °C with. Later, lung sections were taken into 1X PBS + 0.05% Tween-20 (Sigma Aldrich, Cat#: P5927) washes, and followed by secondary antibody Alexa-Fluor 647 (Life Technologies, Cat#: A21244, 1:150 dilution) incubation for 1 hour at room

temperature (24 °C) before starting to go to counter staining step with 5 μ M SYTOX blue nucleic acid stain (Fisher Scientific, Cat#S11348). After counterstaining, slides were washed with distilled water, and they were covered by Immu-Mount fluorescent mounting media to preserve the immunofluorescent character of the staining (Epredia, Cat#: 9990402). A comprehensive list of all immunofluorescent antibodies used for immunofluorescence staining can be found in Table 4.

A comprehensive list of the immunofluorescent antibodies used in this thesis study immunofluorescence staining can be found below (Table 4).

Table 4 Antibodies used for immunofluorescence staining

Target	Antibody	Clone	Host	Dilution	Catalog no.	Company
PCNA, Nuclear non-histone protein	PCNA (proliferating cell nuclear antigen) antibody	Polyclonal	Rabbit	1:100	NB100-456	Novus Bio
N/A (Secondary antibody)	Goat anti-Rabbit IgG (H+L) Alexa-Fluor 647	53.6.72	Goat	1:150	A21244	Life Technologies
Nucleic acids	SYTOX blue nucleic acid stain	N/A	N/A	5 μ M/Sample	S11348	Fisher Scientific

3.12 Confocal microscopy

Images of PCNA and SYTOX Blue stained lung microscopic tumor nodules at a higher power were acquired on a Leica-TCS SP5 confocal microscope (Leica Microsystems, Concord, ON).

3.13 *In vivo* immune cell depletion

In vivo depletion antibodies were dissolved in sterile 1X PBS and applied via intraperitoneal (i.p.) injection to deplete CD4 T cells (clone GK1.5, 500 μ g/injection), CD8 T cells (clone 53.6.72, 500 μ g/injection), and NK cells (clone PK136, 500

µg/injection) immune cell types at sixth and eighth weeks of NNK administration. The control group was administered by an i.p. vehicle (sterile saline). To check the adverse effects of *in vivo* antibodies, during the follow-up of the animals, animal health status was evaluated once a week by checking their clinical status (with physical examination) and measuring their body weights. A comprehensive list of all the antibodies used for *in vivo* depletion of CD4+ T cells, CD8+ T cells, and NK1.1+ NK cells can be found in Table 5.

A comprehensive list of the antibodies used in this thesis study *in vivo* depletion can be found below (Table 5).

Table 5 Antibodies used for *in vivo* depletion antibodies

Target	Antibody	Clone	Injected amount	Catalog no.	Company
CD4 T cells	Anti-mouse CD4 antibody	GK1.5	500 µg/injection	NB100-456	Bio X Cell
CD8 T cells	Anti-mouse CD8 antibody	53.6.72	500 µg/injection	S11348	Bio X Cell
NK cells	Anti-mouse NK1.1 antibody	PK136	500 µg/injection	A21244	Bio X Cell

3.14 Peripheral blood processing and staining for flow cytometric analysis of *in vivo* depletion.

For the flow cytometry analysis of the *in vivo* depletion status of the experimental groups, peripheral blood samples were taken from the submandibular vein at 72 hours and 12 weeks post-*in vivo* antibody injections. Mice were handled, and an 18G needle was used to make a small puncture to the submandibular vein. 3–4 drops of blood (100 µl) were collected in a heparin-covered tube, mixed well, and transferred on ice. After the collection of blood, light pressure was applied using a sterile cotton piece to the vein to stop bleeding. Mice were followed taking blood samples to guarantee no adverse events occurred. 100 µl of peripheral blood from each depletion group mouse and a minimum of one animal from non-depleted

groups were added into separate fluorescence-activated cell sorting (FACS) tubes (Falcon, BD). Peripheral blood samples were used for the confirmation of the depletion of targeted immune cell populations defined for each experimental group. Anti-CD3-V500 (BD Bioscience, Cat#: 560,771), anti-CD4 Alexa-Fluor 700 (BD Pharmingen, Cat#: 557956, clone RM4-5), anti-CD8-APC-Cy7 (BD Pharmingen, Cat#: 557654), anti-NK1.1-APC (BD Bioscience, Cat#: 550627) and 7AAD (BD Pharmingen, Cat#: 51-68981E) fluorescent-conjugated antibodies were added to evaluate depletion of CD4+ T cells, CD8+ T cells and NK1.1+ NK cells. All antibodies were incubated in the dark, at 4°C for 30 minutes with a total cell suspension of 100 µl, using FACS tubes. After several washes with 1X PBS, samples were run in flow cytometry. Cells were separated using 7AAD, and 10000–20000 cells were collected from the live cells gate. A comprehensive list of all flow cytometry antibodies used for flow cytometry can be found in Table 6.

A comprehensive list of the flow cytometry antibodies used in this thesis study peripheral blood immunophenotyping can be found below (Table 6).

Table 6 Antibodies used for peripheral blood immunophenotyping

Target	Antibody	Host	Fluorophore type	Fluorophore Ex/Em	Clone	Catalog no.	Company
CD3 cells	Anti-CD3 antibody	Syrian hamster	V500	415/500 nm	500A2	560771	BD Bioscience
CD4 T cells	anti-CD4 antibody	Rat	Alexa Fluor 700	697/719 nm	RM4.5	557956	BD Pharmingen
CD8 T cells	anti-CD8 antibody	Rat	APC-Cy7	651/779 nm	53-6.7	557654	BD Pharmingen
NK cells	anti-NK1.1 antibody	Rat	APC	651/660 nm	PK136	550627	BD Bioscience
Dead cells	7AAD (7-Amino-Actinomycin D)	N/A	N/A	546/647 nm	N/A	51-68981E	BD Pharmingen

3.15 Lung and lung draining lymph nodes processing and staining for flow cytometry and immunophenotyping.

Lung tissue was dissected from each animal, mechanically dissociated, and transferred to ice for tissue processing. Lung tissue was minced and dissociated with 0.5 mg/ml Type IV Collagenase (Worthington Biochemical, Cat#: 4186) by incubation of a shaker, shaking continuously (New Brunswick Scientific, I-24 incubator Shaker Series) for 40 minutes in 37°C. After digestion, lung tissues were filtered through a 40-µm nylon cell strainer (pluriStrainer, Cat#: 43-50,050-01) to have single-cell suspensions. Lung-draining lymph nodes were dissociated from peripheral excessive tissues mechanically and capsule of the lymph node with a frosted side of glass slides (GSC International, Cat#: 1201A72), and tissue was passed through an 18 G 1 ½ needle (BD PrecisionGlide Needle, Cat#: 305,195) attached to a 10-cc syringe (BD, Cat#: 303,134), to provide a single cell suspension. The single-cell suspension was filtered through a 100-µm nylon mesh (Elko, Cat#: 03–100/32) into FACS tubes. The single-cell isolate suspensions from lung and lung-draining lymph nodes were gone to two PBS washes, and total live cell numbers were counted with trypan blue dye. From each animal, 1 million lung-draining lymph node cell suspensions and 2–3 million lung infiltrating cell suspensions were taken and mouse BD Fc Block (anti-mouse CD16/CD32; BD Pharmingen, Cat#: 553,142, Clone: 2.4 G2) was added. Cell suspensions were incubated in the dark, at 4 °C for 15 minutes. Lung infiltrating cells and lung-draining lymph node cells were stained to be classified based on their specific cell markers for 30 minutes, in the dark at 4 °C. A comprehensive list of all antibodies used for flow cytometry can be found in Table 7.

A comprehensive list of the flow cytometry antibodies used in this thesis for lung and draining lymph node immunophenotyping is shown in Table 7.

Table 7 Antibodies used for lung and draining lymph node immunophenotyping.

Antibody	Host	Fluorophore type	Fluorophore Ex/Em	Dilution	Clone	Catalog no.	Company
Anti-CD3 antibody	Syrian hamster	V500	415/500 nm	1:50	500A2	560771	BD Biosciences
anti-CD4 antibody	Rat	BUV496	348/496 nm	1:200	GK1.5	612952	Biolegend
anti-CD8 antibody	Mouse	SparkViolet538	396/538 nm	1:80	QA17A07	155019	Biolegend

anti-CD11b antibody	Rat	PerCP Cy5.5	488/676 nm	1:100	M1/70	550993	BD Pharmakon
anti-CD11c antibody	Armenian hamster	Alexa Fluor 647	633/668 nm	1:100	N418	117312	Biolegend
anti-CD19 antibody	Rat	BV570	405/570 nm	1:50	6D5	115535	Biolegend
anti-CD25 antibody	Rat	PE/Cy5	488/561 nm	1:200	PC61	102010	Biolegend
anti-CD44 antibody	Rat	BB700	485/693 nm	1:60	IM7	566506	BD Biosciences
anti-CD45 antibody	Rat	APC Fire810	650/810 nm	1:150	30-F11	103174	Biolegend
anti-62L antibody	Rat	BV711	405/711 nm	1:400	MEL-14	104445	Biolegend
anti-107a antibody	Rat	PE/Cy7	488/780 nm	1:800	1D4B	560647	BD Biosciences
anti-PD-1 antibody	Rat	APC	594/633 nm	1:200	29F.1A12	135210	Biolegend
Anti-NKp46 antibody	Rat	BUV737	350/737 nm	1:30	29A1.4	612805	BD Biosciences
Anti-NK1.1 antibody	Mouse	Alexa Fluor 700	633/719 nm	1:800	PK136	108730	Biolegend
Anti-Ly6C antibody	Rat	BV605	405/603 nm	1:20	HK1.4	128036	Biolegend
Anti-Ly6G antibody	Rat	BUV395	348/395 nm	1:100	1A8	563978	BD Biosciences

Anti-F4/80 antibody	Rat	Pacific Blue	405/455 nm	1:100	BM8	123124	Biolegend
Anti- $\gamma\delta$ T-Cell Receptor antibody	Rat	BUV563	350/564 nm	1:50	V65	749464	BD Biosciences
LIVE/DEAD Fixable Blue Dead Cell Stain	Rat	LIVE/DEAD	350/450 nm	1:400	N/A	L23105	Fisher Scientific

3.16 Flow cytometry

Peripheral blood cells, lung and draining lymph node immune cells were analyzed by a Cytex Aurora flow cytometer by collecting and sorting the cells from live CD45+ leukocytes population. After flow cytometry, the data was analyzed to calculate cell percentages and absolute cell numbers. The data was statistically analyzed using a one-way ANOVA in GraphPad software, v.9. A comprehensive list of the flow cytometry antibodies to classify lymphoid/ myeloid populations is shown in Table 8. An example of the gating strategy of the cell populations used in FCS Express v.7 (De Novo Software, CA) is shown in Figure 5. First, cells were sorted by using FSC-A (forward scatter) and SSC-A (side scatter) based on their size and granularity and defined cells with their previously shown features (78) also, debris was eliminated. Second, by using FSC-A/FSC-H gating and SSC-A/SSC-H gating cell doublets and clumps were eliminated from the population. Total live cell populations are then sorted with the exclusion of a Live/Dead dye. From live cells, leukocytes were identified with their CD45 expression. T and B lymphocytes were separated from all leukocyte populations based on their CD3 expression (T lymphocytes) and CD19 (B lymphocytes) markers. From the CD3+ T lymphocyte population, CD4+ T cells and CD8+ T cells were identified. These gating principles were applied to the cell populations mentioned in Table 8. The subsequent gating was used to define even the small populations to investigate the immunomodulatory effects of SA-4-1BBL in the spontaneous preclinical lung cancer model.

A comprehensive list of the flow cytometry antibodies used in the lung and draining lymph node immunophenotyping to classify lymphoid/ myeloid panel is shown in Table 8.

Table 8 Antibodies used for lung and draining lymph node immunophenotyping lymphoid/myeloid panel.

Antibody	Fluorophore type	Dilution	Cell type
Anti-CD3 antibody	V500	1:50	T cells
anti-CD4 antibody	BUV496	1:200	CD4+ T cells
anti-CD8 antibody	SparkViolet538	1:80	CD8+ T cells
anti-CD11b antibody	PerCP Cy5.5	1:100	Myeloid cells
anti-CD11c antibody	Alexa Fluor 647	1:100	Dendritic cells
anti-CD19 antibody	BV570	1:50	B cells
anti-CD25 antibody	PE/Cy5	1:200	Regulatory T cells
anti-CD44 antibody	BB700	1:60	Effector memory T cells
anti-CD45 antibody	APC Fire810	1:150	Leukocytes
anti-62L antibody	BV711	1:400	Naïve and central memory T cells
anti-107a antibody	PE/Cy7	1:800	Cytotoxic cells (CD8+ T cells and NK cells)
anti-PD-1 antibody	APC	1:200	Activated and exhausted T cells
Anti-NKp46 antibody	BUV737	1:30	NK and NKT cells

Anti-NK1.1 antibody	Alexa Fluor 700	1:800	NK and NKT cells
Anti-Ly6C antibody	BV605	1:20	Monocytes
Anti-Ly6G antibody	BUV395	1:100	Neutrophils
Anti-F4/80 antibody	Pacific Blue	1:100	Macrophages
Anti- $\gamma\delta$ T-Cell Receptor antibody	BUV563	1:50	γ/δ T cells
LIVE/DEAD Fixable Blue Dead Cell Stain	LIVE/DEAD	1:400	Dead cells

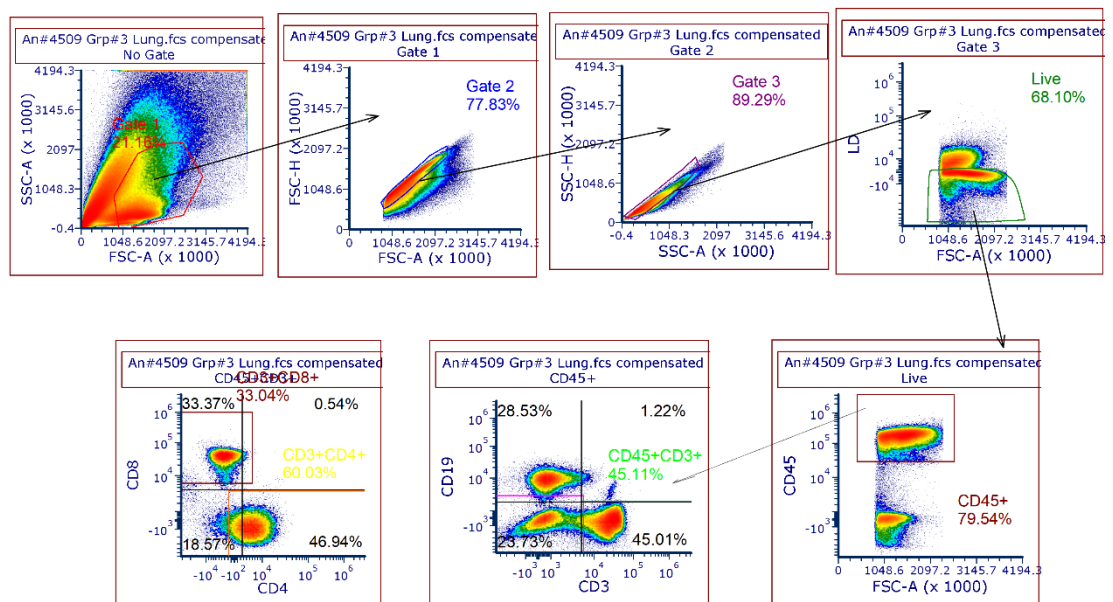


Figure 5. The main gating strategy to classify cell populations in FCS Express software.

3.17 Statistical analyses

Statistical analyses were conducted by using GraphPad Prism v.9 software (La Jolla, CA). To determine significant differences between groups, Student's t-tests and

one-way ANOVA tests were used. More, two-way ANOVA was used to investigate the effects of two different variables, treatment (NNK vs. NNK + SA-4-1BBL) and time. To assess the body weight changes between different treatment groups two-way ANOVA test was used. All p-values ≤ 0.05 were stated as statistically significant.

4. FINDINGS

4.1 NNK administration-induced lung tumorigenesis in A/J mice

Lung tumor induction is one of the preclinical models and is frequently used to have the translational model for lung cancer patients with long-time smoke exposure and tobacco usage. It can be induced by exposing animals to pro-carcinogenic chemical components of tobacco smoke. Animals can be exposed mainly by using smoke chambers, intragastric gavage, nicotine patches, or intraperitoneal injections of the carcinogens in predetermined periods. These models promise a better model to enlighten the lung cancer pathogenesis and modulate the diverse therapeutic and preventive approaches against it. To determine if the administration of immunomodulatory molecules to mice exposed to carcinogenic chemicals, macroscopic and microscopic tumor nodule formations in lungs were evaluated using a dissecting microscope and histopathological analyses. To observe the immunomodulatory effects of the SA-4-1BBL molecule in mice models, the A/J mice strain was chosen, due to their increased potential to induce lung tumors under nicotine-derived chemical exposure. This feature makes them one of the main strains in use for preclinical lung cancer models (68,72,73,79,80). A/J strain of mice are susceptible to develop spontaneous lung tumors due to an alteration in the PAS1 gene, linked to the KRAS proto-oncogene (81). The KRAS proto-oncogene modulates cell proliferation, and mutations in the PAS1 gene are involved with the pathogenesis of distinct cancers, like lung cancer. In this thesis study, one type of nitrosamine, NNK (4-(Methylnitrosamino)-1-(3-pyridyl)-1-butanone), was preferred due to its carcinogenic potential. Previous studies have shown that NNK is the most effective carcinogenic nicotine compound in humans and different species of animals, to induce lung cancer (72,73,79). In the preliminary experiments, 10 μmol NNK was administered using intragastric gavage into A/J mice in the first eight weeks of the follow-up. Animals were followed up for 42 weeks and terminated to evaluate lung tumor nodule formation. In this setting, lung tumor nodules were visible in their lungs. Whereas follow-up after NNK injection was a long time frame and the study design needed to be optimized and modified. Thus, induction of lung tumorigenesis was expedited by administrating NNK via i.p. injection, by 25 mg/kg weekly dose for eight consecutive weeks (68). Naïve A/J mice received a PBS injection instead of an NNK injection. In the sixth- and eighth after NNK administrations, the SA-4-1BBL molecule was injected subcutaneously (Figure. 6). Mice were observed at the beginning of each week for 18 weeks to evaluate any changes in the animals' clinical health status posterior to receiving NNK and SA 4-1BBL injections based on their experimental groups. Body weight changes of the NNK+ SA-4-1BBL treatment group

did not show any significant changes compared to the untreated age-matched control group (Figure 7). At the endpoint of the study, animals were terminated and organs (kidney, liver, bladder, stomach, etc.) were evaluated to analyze NNK and/or SA 4-1BBL treatment-related adverse pathologies. The control group (NNK+ Vehicle) received a PBS i.p. injection in weeks 6 and 8. There were no significant differences between the treatment (NNK+SA-4-1BBL) and control (NNK+ Vehicle) groups (data not shown), and this supported the previous findings about the safety profile of SA-4-1BBL treatment (31,32,37,38,55–58,61,62).

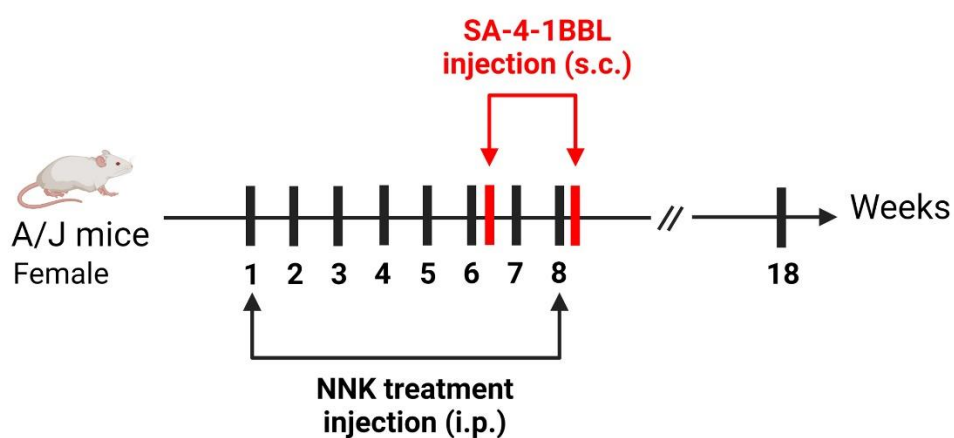


Figure 6. Treatment scheme of A/J mice to evaluate the carcinogenic effects of NNK and immunomodulatory effects of SA-4-1BBL.

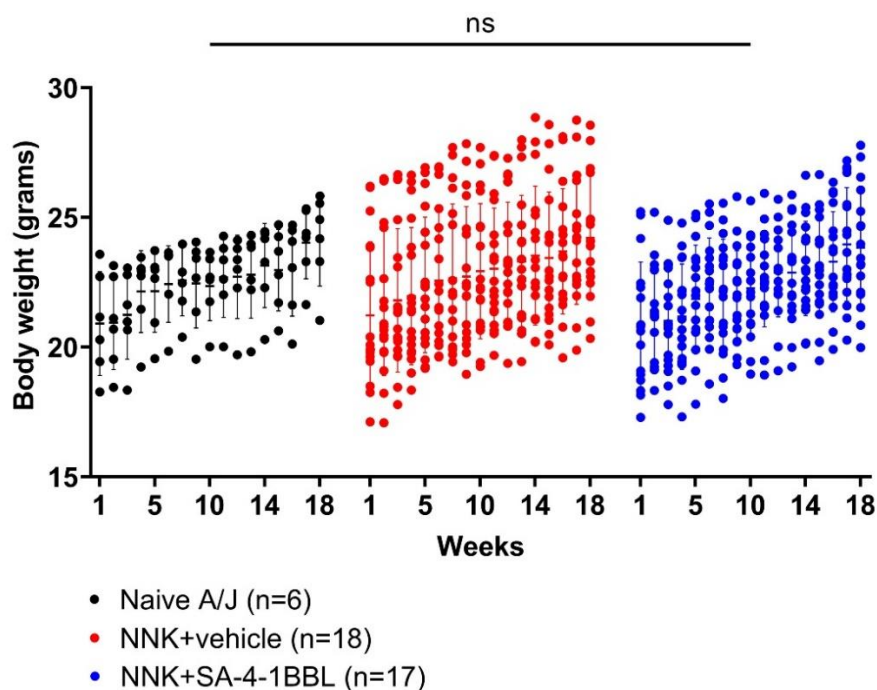
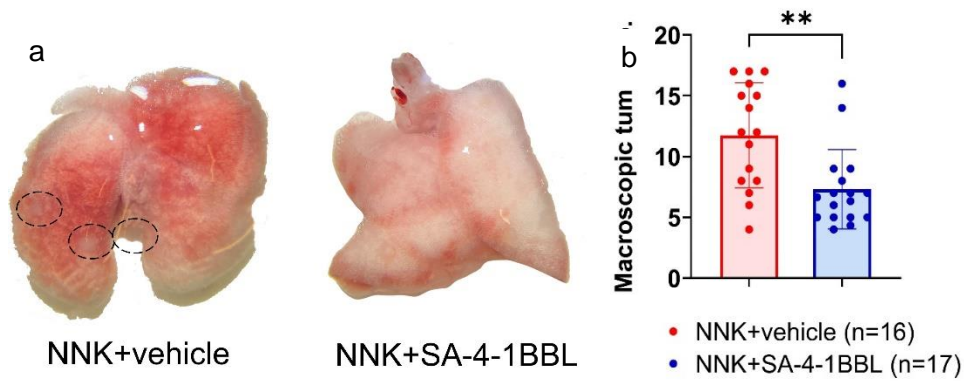


Figure 7. Body weights of the animals during the 18-week follow-up.

4.2 SA-4-1BBL Treatment Significantly Limited the Tumor Nodule Formation in Long-Term NNK- Exposed A/J Mice Model.

In previous studies, SA-4-1BBL was an effective and safe molecule with an immunomodulatory nature against various subcutaneously injected tumors, such as cervical cancer and lung cancer in mouse models (62). These findings were promising, considering that pretreatment with SA-4-1BBL molecule was efficient in distinct cancer types without a need for antigenic priming. Considering this information, in this thesis study, the efficacy and modulator effects of the SA-4-1BBL were investigated in the NNK-induced lung cancer preclinical model. One of the purposes of this thesis project was to assess the inhibitory effect of SA-4-1BBL against NNK-induced lung tumorigenesis. In weeks six and eight weeks of NNK administrations, 100 μ g of SA-4-1BBL was applied to animals subcutaneously (Figure 6). After following mice for 18 weeks, mice were euthanized to analyze the effects of SA-4-1BBL monotherapy. After harvest and perfusion, lungs were put into a tissue dish, and macroscopic tumor nodule formation was evaluated by two investigators, independently and blinded to experimental groups. Macroscopic tumor nodule formation was observed on the lung surface, using a dissecting microscope. In these observations, mice receiving SA-4-1BBL monotherapy showed significantly fewer macroscopic tumor nodules than the NNK + vehicle control group (Figures 8a and 8b).

The preventive efficacy of SA-4-1BBL monotherapy was consistent among repeated experiments with the same settings. This finding suggested the potential of immune checkpoint stimulation. Opposite to the clinical presentation of lung cancer in humans, macroscopic tumor nodule formation was in peripheral parts of the lungs (Figure 8a, black circles).



Figures 8a and 8b. Macroscopic tumor nodules (Figure 8a., left), and macroscopic tumor nodule numbers in SA-4-1BBL treated and non-treated groups (Figure 8b., right).

Macroscopic tumor nodules need to be confirmed further to be defined as neoplasm by histopathological analyses. Thus, parts of the lungs were taken into H&E staining. Stained slides were analyzed based on their microscopic tumor nodule formation by counting the tumor foci using a bright field microscope. Each slide was evaluated, and microscopic tumors were assessed independently by two experienced investigators, blinded to experimental groups. In parallel with the clinical approach, PCNA staining was utilized to evaluate the proliferative capacity of observed microscopic tumor nodules (Figure 9).

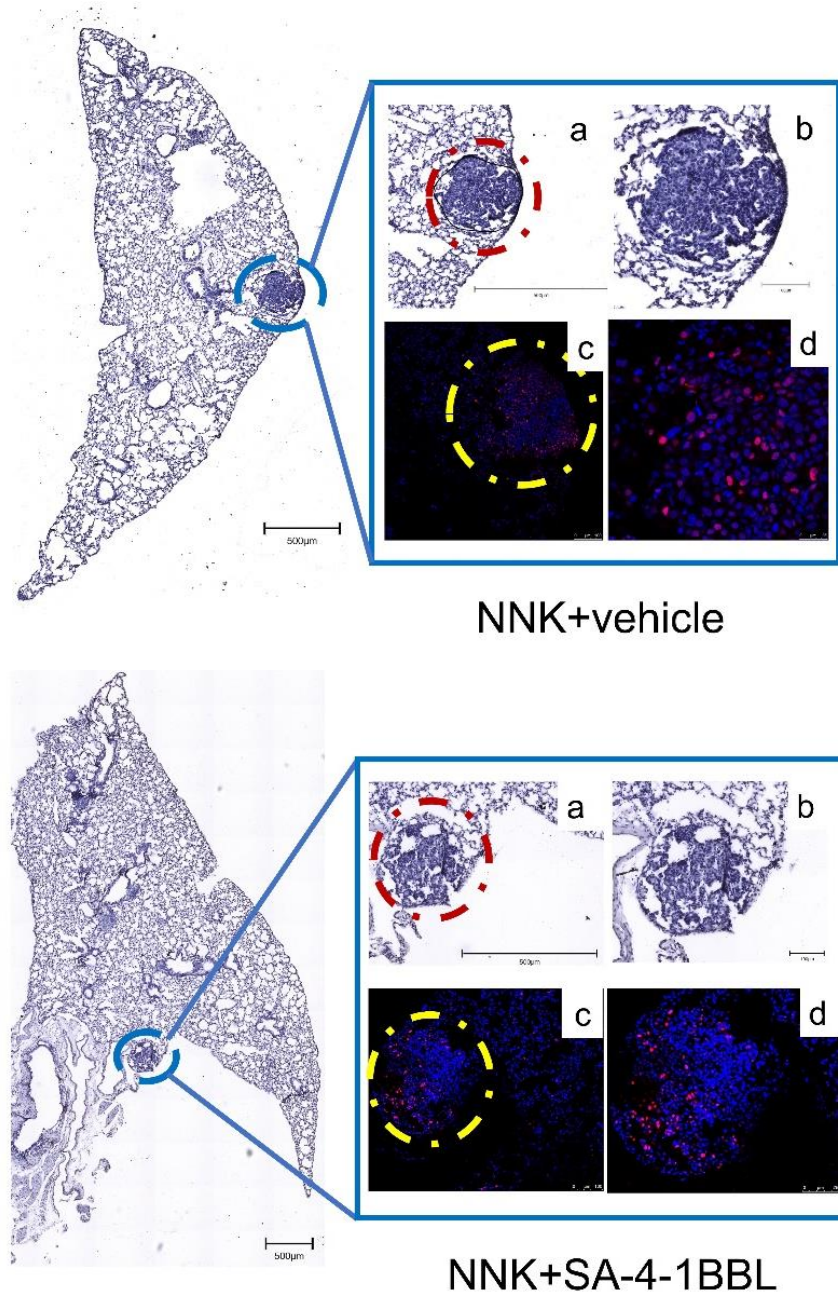


Figure 9. PCNA staining in SA-4-1BBL treated and non-treated lungs.

SA-4-1BBL monotherapy received mice group showed significantly lower amounts of microscopic tumors than the NNK + vehicle control group (Figure 10). Furthermore, in one mouse from the SA-4-1BBL administered group, microscopic tumor nodules were not observed. This promising protection against microscopic tumor nodule formation in the lungs can be attributed to the boosted immunomodulatory effects of SA-4-1BBL treatment. Effects of SA-4-1BBL may be increased due to previous administration and supporting the modulator effects in the second exposure. To evaluate the effects of SA-4-1BBL on the proliferation capacities

of tumor cells, microscopic tumor nodule sizes were measured by analyzing nodules from digital microscopy images (Figures 11 and 12).

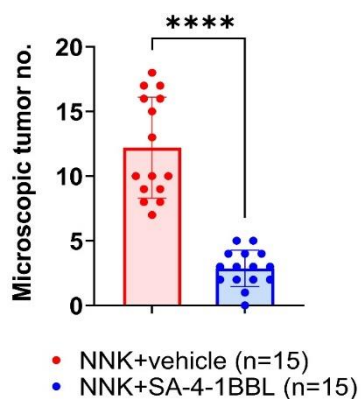


Figure 10. Microscopic tumor nodule numbers in SA-4-1BBL treated and non-treated groups.

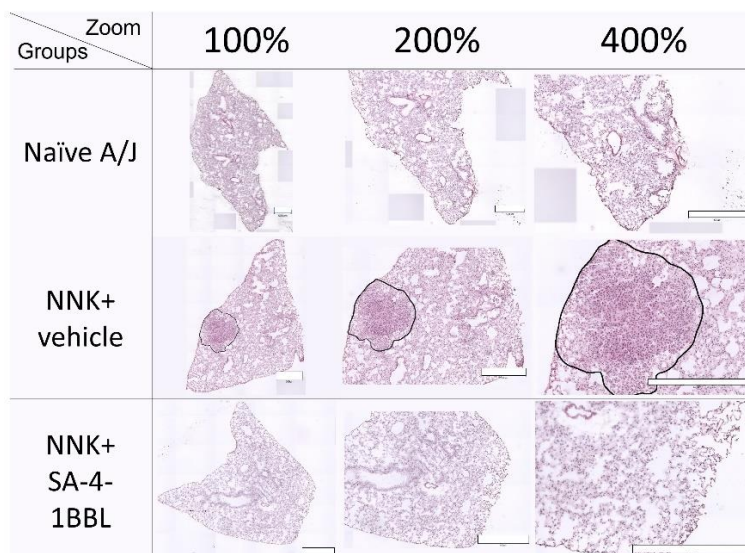


Figure 11. Digital microscopy images of hematoxylin and eosin stained lung sections.

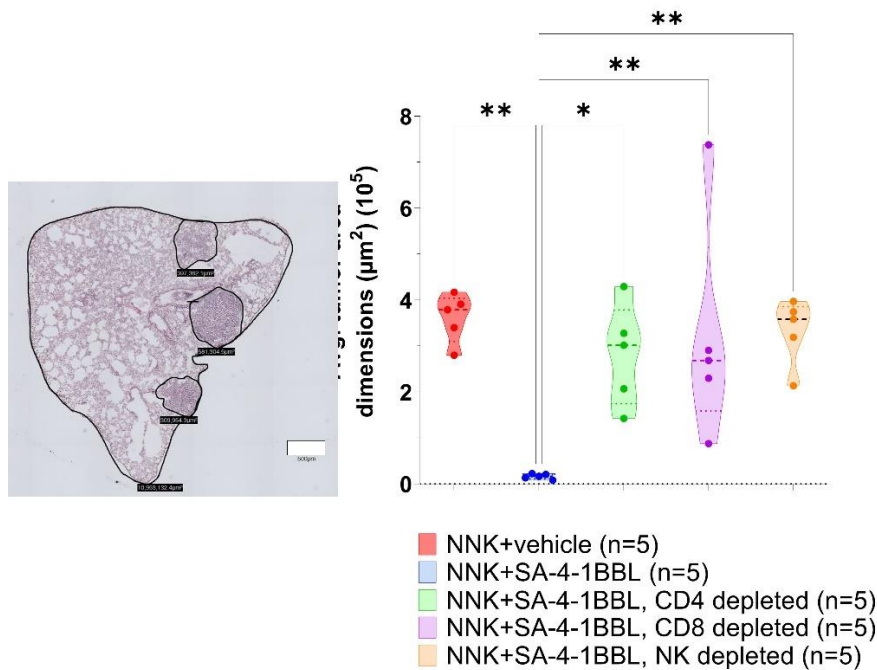


Figure 12. Tumor area measurement of microscopic tumor nodules from each lung section.

Microscopic tumor nodule sizes and the percentage of tumoral area in whole lung sections were analyzed for this evaluation. Microscopic tumor sizes and tumor percentages inside lung tissue were significantly smaller in the SA-4-1BBL treated mice than the ones in the NNK + vehicle control group (Figures 12 and 13).

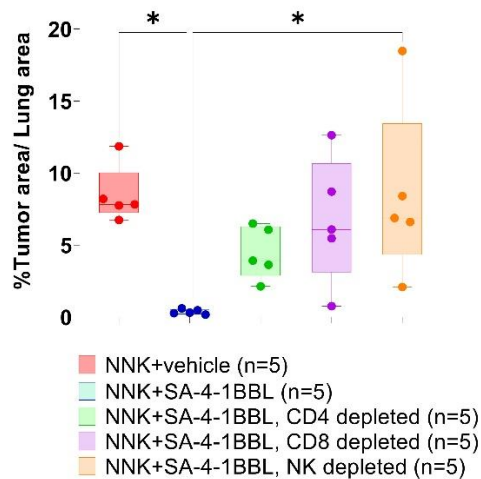


Figure 13. Percentages of microscopic tumor nodule areas to total lung areas between different treatment groups.

4.3 CD4, CD8 T Cells and NK Cells Were Essential Players for SA-4-1BBL Mediated Prevention Against NNK- Induced Lung Cancer.

In past studies, preventive outcomes of SA-4-1BBL were evaluated, and this effect was shown to be dependent on cross-communication between CD4⁺CD44^{high} “memory-like” T lymphocytes and NK cells, with a necessity of synthesized IFN- γ by memory-like T cells located in the environment (62). Based on this background information, it was inevitable to investigate which immune cell population/s is/are responsible for the protective and modulator effects of SA-4-1BBL in the NNK-induced lung tumor model. Thus, with the same settings of NNK and SA-4-1BBL administration, some mice were separated, and *in vivo* depletion of distinct immune cell populations was performed. Depletion antibodies with *in vivo* activity and reactivity for CD4⁺, CD8⁺, and NK immune cell populations were simultaneously administered into depletion group animals via intraperitoneal injection in weeks six and eight of NNK injections as illustrated in Figure 14.

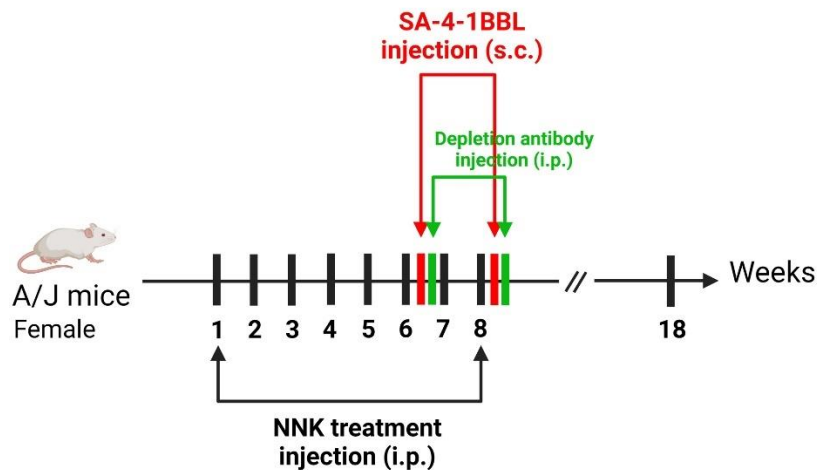


Figure 14. Experimental design of SA-4-1BBL treated and non-treated A/J mice with or without *in vivo* antibody administration.

To investigate the possible adverse effects of *in vivo* depletion antibodies, animals were followed up using their clinical status and body weights. *In vivo* cell depletion did not cause any difference between experimental groups (Figure 15). The mentioned doses of *in vivo* depletion antibodies were enough to cause the CD4 and CD8 lymphocyte depletion (Figures 16a and 16b).

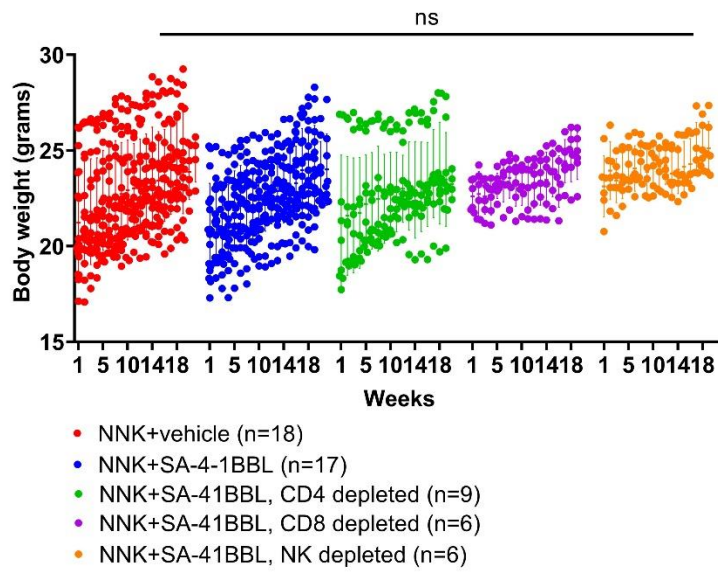
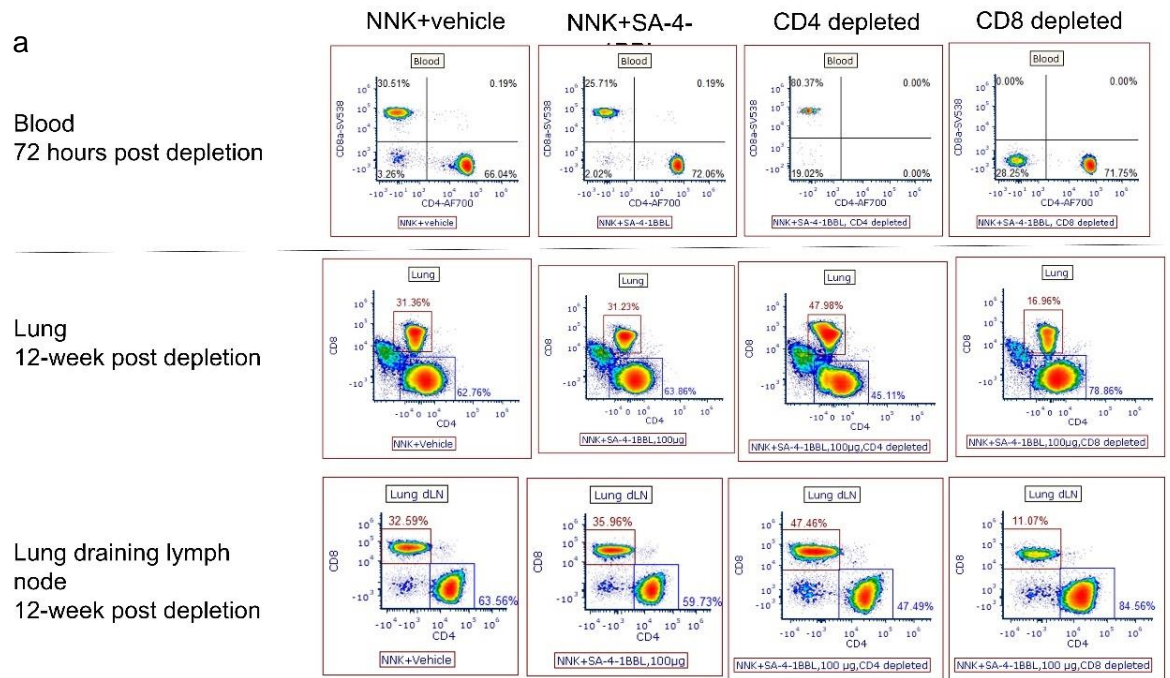
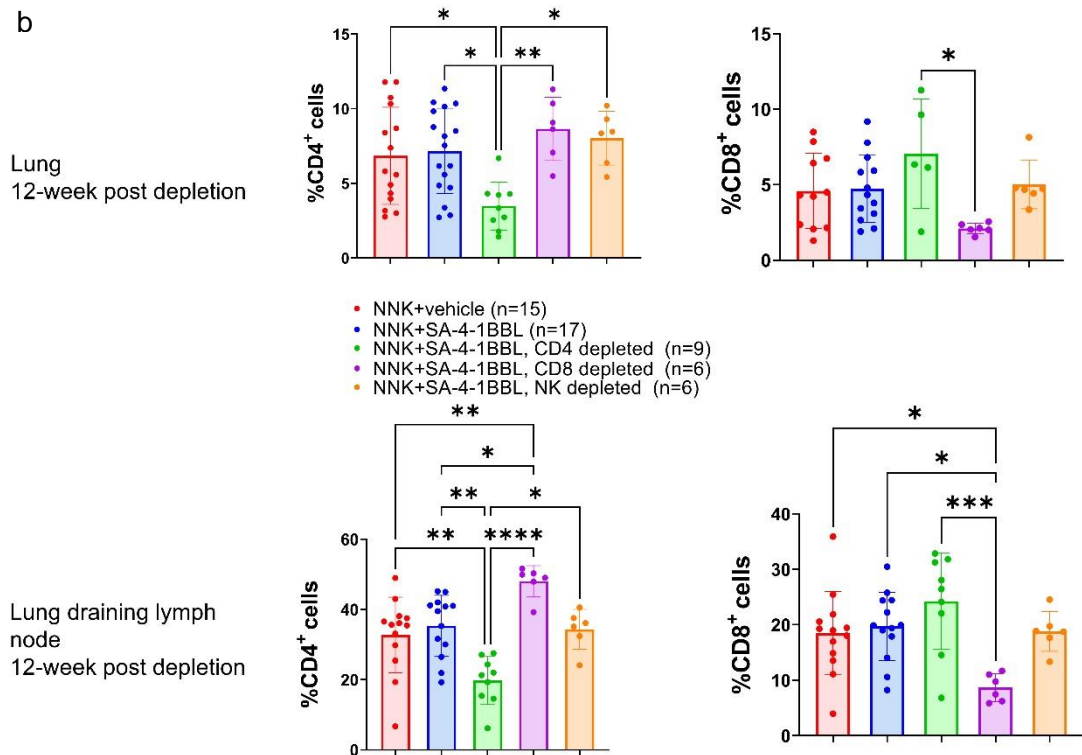


Figure 15. Body weights of the animals with or without SA-4-1BBL and *in vivo* immune cell depletion during the 18-week follow-up.





Figures 16a and 16b. CD4⁺ and CD8⁺ T lymphocyte populations in non-depleted and *in vivo* depletion antibodies administered groups' peripheral blood, lung, and lung draining lymph node samples at 72 hours and 12 weeks post depletion.

In vivo depletion of CD4⁺ T cells, CD8⁺ T lymphocytes, and NK cells abolished the protection effect of the SA-4-1BBL monotherapy. In the CD4⁺ T cells depleted group (Figure 16a and 16b), a significant escalation in both macroscopic and microscopic tumor nodule formation was seen in comparison to mice that did not receive CD4⁺ T lymphocytes depleting antibodies (Figure 17, 18, 19). On the other hand, *in vivo* depletion of CD8⁺ T lymphocytes (Figure 16a and 16b) and NK (natural killer) cells led to a significant escalation in microscopic tumor nodule formation, but no significant alteration was observed in macroscopic tumor nodule formation (Figure 17, 18, 19). In this manner, the mentioned findings suggest that CD4⁺ T lymphocyte contribution is essential to establish the antitumoral immune responses, and this finding is parallel with the past study performed using SA-4-1BBL (62).

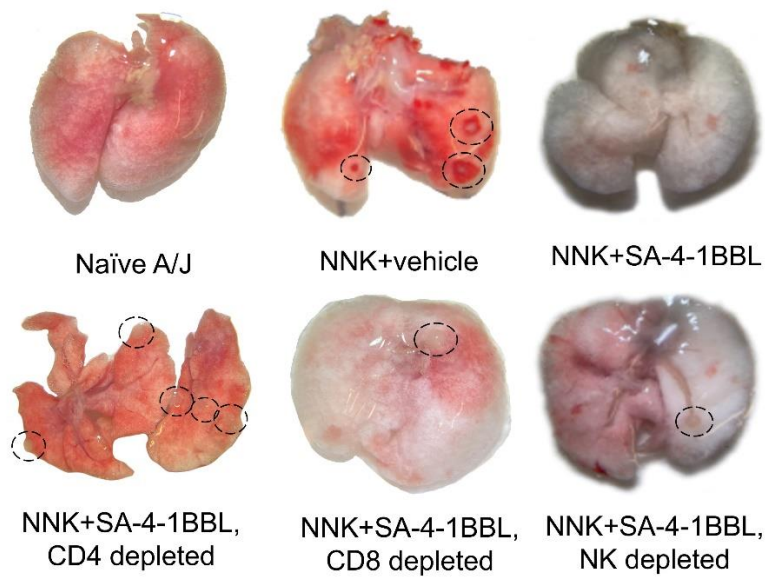


Figure 17. Macroscopic tumor nodules (black circles) in different groups with or without SA-4-1BBL therapy and *in vivo* immune cell depletion.

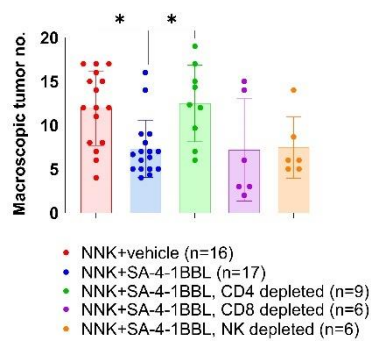


Figure 18. Macroscopic tumor nodule numbers in different groups with or without SA-4-1BBL therapy and *in vivo* immune cell depletion.

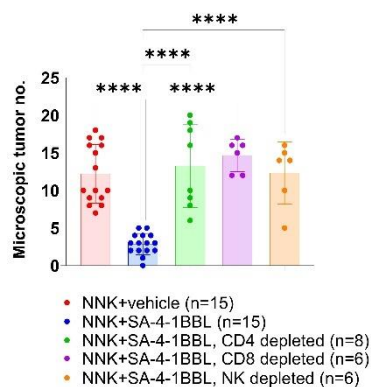
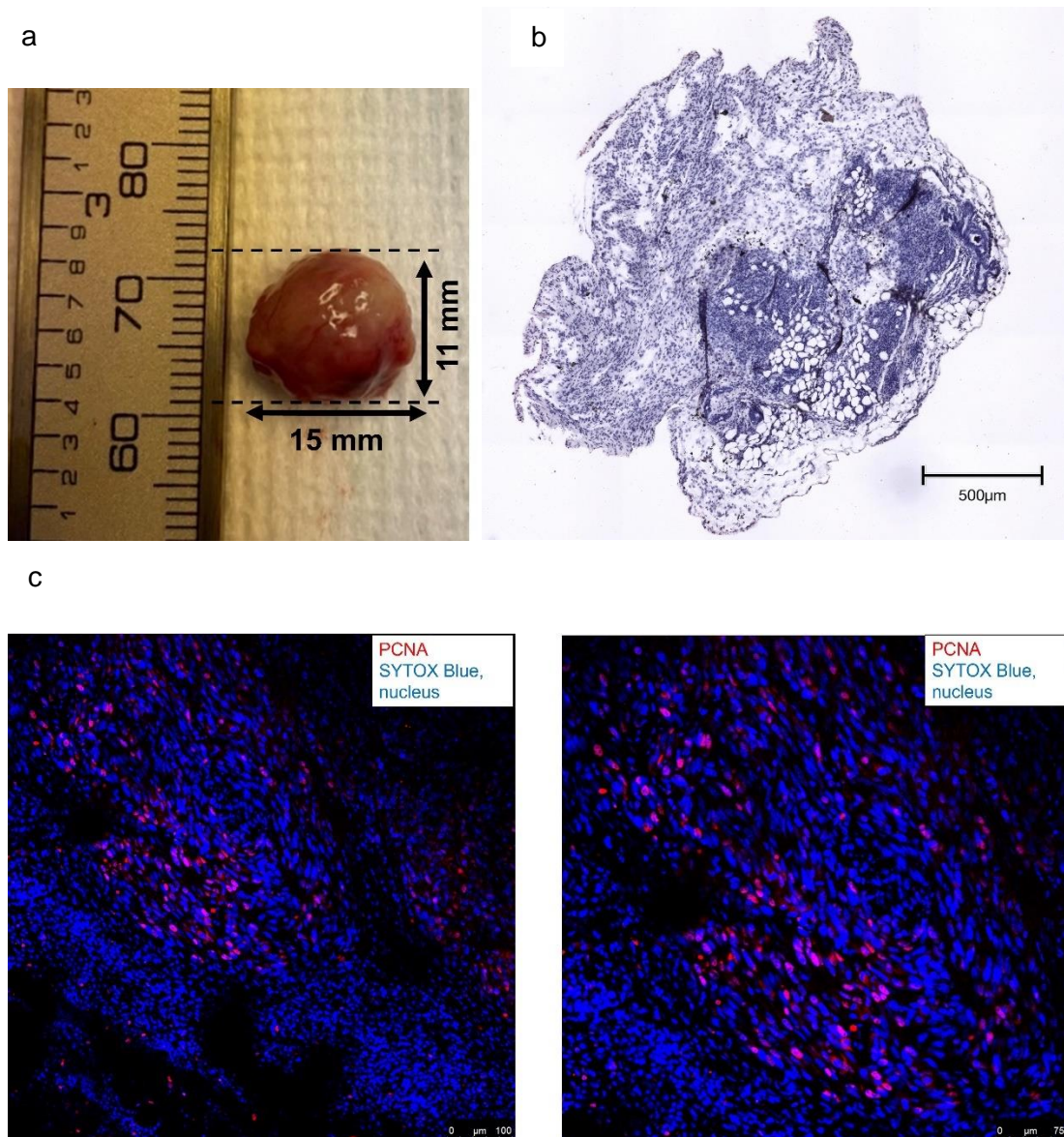


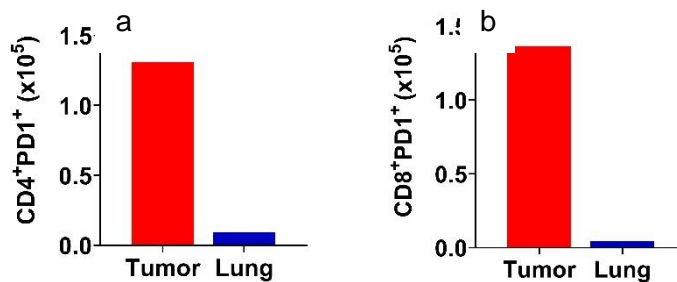
Figure 19. Microscopic tumor nodule numbers in different groups with or without SA-4-1BBL therapy and *in vivo* immune cell depletion.

Due to the nature of carcinogen-induced cancer models, developing metastasis or tumorigenesis in various organs was possible. Hence, on the day of termination, mice were evaluated in a detailed manner and all the organ systems were checked for metastasis and tumor formation. In this evaluation under a dissecting microscope, tumor burden was limited to the lungs. Strikingly, one mouse from the *in vivo* CD4+ T lymphocytes depleted group showed a mass similar to a metastatic focus close to its mandibula. On the termination day, this lesion was removed, and tissue was collected for flow cytometry and histopathological analyses. Analyses showed that the tumoral lesion was metastatic, and it had the same histopathological phenotypes as the ones observed in the lungs (Figures 20a, 20b, 20c).



Figures 20a, 20b and 20c. The mass dissected from the chin of an animal from the CD4+ cells depleted group (Figure 20a), hematoxylin and eosin staining (Figure 20b), and PCNA staining of the same tissue (Figure 20c).

In the flow cytometry analysis of tumor-infiltrating leukocytes, the mass showed 14-fold augmentation in PD1+ CD4+ T lymphocytes and PD1+ CD8+ T lymphocytes (PD-1, programmed cell death protein 1) than the lungs with microscopic tumor nodules (Figures 21a and 21b).



Figures 21a and 21b. Immunophenotyping of the mass dissected from the chin of one *in vivo* CD4+ cell-depleted animal. PD1+ CD4+ cells (Figure 21a, left) and PD1+ CD8+ cells (Figure 21b, right) compared with the lung tissues from the same animal.

In contrast to the findings of the effectivity profile of SA-4-1BBL in recently published cell line-derived subcutaneous tumor models, *in vivo* CD8+ T lymphocyte depletion caused a significant abolishing result on the protective effect of SA-4-1BBL monotherapy in an NNK induced mouse model (62). These data indicate that CD8+ T lymphocytes play a crucial aspect in the activity of SA-4-1BBL (Figures 17, 18, 19). In comparison to SA-4-1BBL-treated mice, areas of microscopic tumor nodules had significantly bigger dimensions in the lung of SA-4-1BBL-administered animals depleted of either T lymphocytes or NK (natural killer) cells and were comparable to the NNK control (Figures 12, 13, 22). These data pointed out that the immunotherapeutic activity of SA-4-1BBL employed the attendance of T lymphocytes and NK cells. In general, these results gave a significant perspective into the mechanisms governing the immunotherapeutic effects of SA-4-1BBL monotherapy and pointed out the importance of T lymphocytes and NK cells in the antitumoral immune responses against lung cancer.

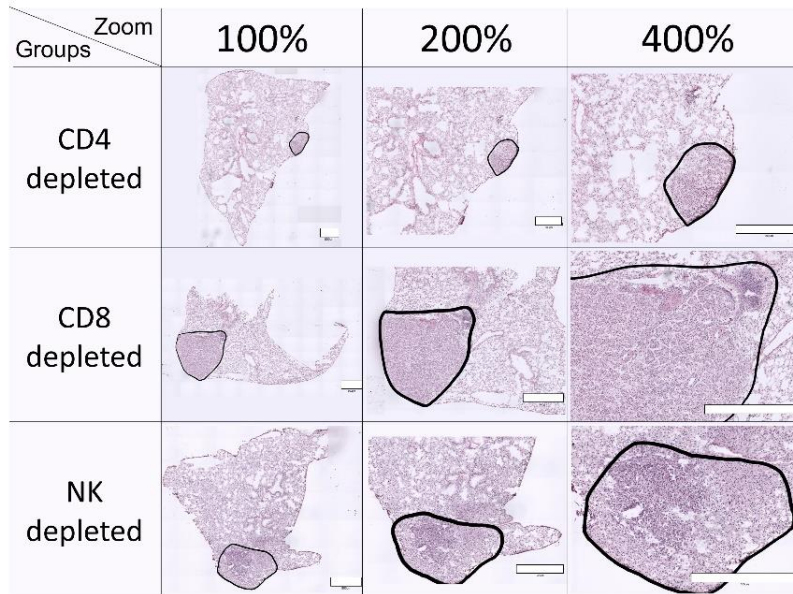
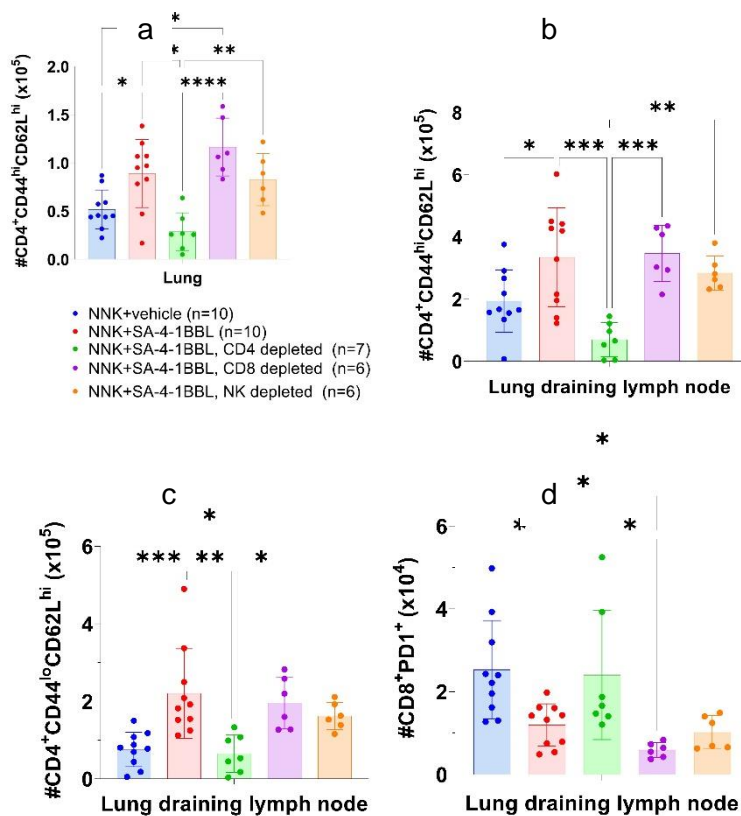


Figure 22. Digital microscopy images of hematoxylin and eosin stained lung sections in *in vivo* cell depletion groups.

4.4 Treatment with SA-4-1BBL monotherapy boosted Central Memory CD4+ T Cells and Naïve CD4+ T Cells and Reduced the Formation of PD-1+ CD8 T Cells.

It has been recently shown that pretreatment with SA-4-1BBL boosted long-term immune memory and was conducted by NK cells and IFN- γ synthesizing CD4+ T lymphocytes (62). Lungs and draining lymph nodes were harvested and processed to isolate tissue infiltrating immune cells to perform deep immune phenotyping. With this analysis, between different treatment groups differences in immune cell populations were compared. Compared with the control group (NNK + vehicle), SA-4-1BBL significantly boosted the absolute cell number of CD4+ central memory T cells (CD4+CD44^{hi}CD62L^{hi}) in lung and draining lymph nodes ($p < 0.05$) (Figures 23a and 23b). With SA-4-1BBL pretreatment, central memory T cells may be activated with tumor antigens in the lungs and lung-draining lymph nodes and stimulated with SA-4-1BBL molecules. Next, with their reentry to secondary lymphoid organs, they may facilitate faster and more effective antitumoral immune responses upon re-exposure to antigens compared with naïve T cells. In the lung draining lymph nodes of the SA-4-1BBL treatment group, the number of naïve CD4+ T lymphocytes (CD4+CD44^{lo}CD62L^{hi}) was significantly higher than the control (NNK + vehicle) group. These naïve CD4+ T cells may have a reservoir for effective and memory T cell formation against tumor cells (Figure 23c). Moreover, in the lung-draining lymph nodes of SA-4-1BBL pretreated animals, with the immunomodulatory effects of SA-

4-1BBL, there was a significant reduction in the absolute cell numbers of PD-1 positive CD8+ T lymphocytes (Figure 23d). The programmed cell death protein 1 (PD-1) receptor is a critical immune checkpoint receptor that is primarily expressed on the cell membranes of activated T cells. Its interaction with its ligands, programmed death-ligand 1 (PD-L1), delivers inhibitory signals that decrease immune activation. This PD-1/PD-L1 binding is exploited by tumor cells in the tumor niche to provide an immune evasion mechanism. PD-1+ CD8+ T lymphocytes may lead to T cell exhaustion in the microenvironment. In various studies performed in NNK-induced lung cancer preclinical animal models, it has recently been shown that lung neoplasms express PD-L1 on their cell membranes (72) (73). Thus, a reduction in PD-1 expressing CD8+ T lymphocytes in the SA-4-1BBL pretreated group can serve as an additional mechanism to support its antitumoral immune modulator effect. Nevertheless, further mechanistic studies are required to prove this interpretation and enlighten the immunomodulatory role of SA-4-1BBL in the NNK-induced spontaneous lung cancer model.



Figures 23a, 23b, 23c and 23d. CD4⁺ central memory T lymphocytes (CD4⁺CD44^{hi}CD62L^{hi}) in lungs (Figure 23a), and lung draining lymph nodes (Figure 23b), naïve CD4⁺ T lymphocytes (CD4⁺CD44^{lo}CD62L^{hi}) in (Figure 23c), and PD1⁺ CD8⁺ cells (Figure 23d) in lung draining lymph nodes of the animals with or without SA-4-1BBL and *in vivo* cell depletions.

5. DISCUSSION

The encompassing purpose of this thesis study was to assess the antitumoral efficacy of a promising immunomodulatory molecule, SA-4-1BBL, in a nicotine-induced spontaneous lung cancer preclinical model. To our knowledge, this is the first study to show that spontaneous lung cancer can be prevented, using an immunomodulatory molecule while analyzing the essential immune cell populations for this activity. For this, there was a need for a mouse strain to be used to reflect the human patient profiles with nicotine exposure for a timeframe. Thus, in this thesis study, we used the A/J mouse strain. A/J mouse strains are known for their genetic susceptibility to nicotine-induced lung cancer (82–84). Thus, they are one of the main mouse strains in use to investigate lung cancer pathogenesis and therapeutic approaches in the preclinical field (85,86). Human lung cancers have a distinct genetic alteration depending on cancer type, other strains can be used to widen the scope of investigations (86). For instance, to investigate the human lung adenocarcinoma with specific genetic alterations (e.g. KRAS mutation), and genetically engineered strains, such as the *Kras^{SL-G12D}* strain (87,88). Scenarios relevant to non-small cell lung cancer patients can be replicated by using transgenic mice strains with EGFR gene mutations (89,90). Immunocompromised strains including NSG mice (NOD SCID gamma) can be used to develop patient-derived xenografts (PDX) models to evaluate the immune cell profiles and pave the way for personalized medicine approaches (85,91). Despite the knowledge that has been gathered from animal studies, challenges persist. Genetic variations between mice and humans require cautious interpretation of findings. For instance, nicotine consumption and smoking are mostly related to squamous cell cancer in the lungs of humans however it causes adenocarcinoma histopathological lung cancer subtype in mice (83). Moreover, smoking-related lung cancers tend to be in the peripheral parts of the lungs in humans, while it is in the peripheral regions of the lungs in mice models. Our study findings were also parallel with previous studies, NNK- NNK-induced tumors were mostly located in peripheral parts of the lungs and the histopathological type was adenocarcinoma. (Figures 11 and 22) Moreover, the complexity of the immune system's role against lung tumorigenesis necessitates a multifaceted approach, incorporating various mouse strains and animal types besides mice to capture diverse aspects of lung cancer biology. Additionally, integrating cutting-edge technologies, such as CRISPR-Cas, can offer further advantages to refine the genetic manipulations in mouse models and provide the progress of preclinical research and clinical trials in lung cancer (92,93). With these modifications, certain mutations can be seen in humans as cf DNA (cell-free DNA) and miRNA can be detected based on the CRISPR/Cas system, which is promising in screening and diagnosing lung cancer (92). In this thesis study, to induce lung cancer with nicotine consumption, first, we tried to administer NNK via intragastric gavage, using 3 mmol/kg as described in the previous studies (94,95). But in this setting, in our study, it took a 42-week period to induce lung cancer formation in mice (data not shown). Thus, we needed to adopt these findings to our project. In this project, considering the long period of tumor induction, we administered 25 mg/kg NNK in intraperitoneal injection for the first eight consecutive weeks.

Importantly, in comparison with the previously reported intragastric gavage technic, in this thesis study, we showed that eight weeks of intraperitoneal injections of NNK were enough to promote lung tumorigenesis in 18 weeks, with a 100% microscopic tumor formation rate. To our knowledge, this is one of the shortest periods shown in the literature, to induce lung tumor formation in A/J mice using NNK. During the ongoing tumorigenesis, the treatment group was administered 100 μ M SA-4-1BBL costimulatory molecule. Our purpose was to evaluate whether treatment with SA-4-1BBL had the potential to stop lung tumorigenesis compared to the group that did not receive it. The dose of SA-4-1BBL was determined based on the previously reported work of our group. 100 μ g SA-4-1BBL is shown as the optimal dose to protect from subcutaneous tumor challenge, and this protection was compromised in the lower doses (62). To our knowledge, this is the first time that an immune costimulatory molecule used to modulate the immune system in nicotine-induced spontaneous lung cancer formation in a preclinical model. Since this study had a different nature of tumor formation than injected tumor models by being a spontaneous cancer model, and the possible differences between mouse strains used in the previous study (C57BL/6) versus A/J mice, we needed to use varied levels of doses of SA-4-1BBL to see the optimal immunomodulatory effect. Even though we tested higher levels of doses of SA-4-1BBL (150 μ g), the most efficient administration regimen consisted of two doses of 100- μ g SA-4-1BBL, two weeks apart. The SA-4-1BBL aims at the 4-1BB/ 4-1-BBL interaction and modulates the immune system using this axis. Recent works have highlighted those agonistic antibodies for T-cell costimulatory receptor 4-1BB (CD137) shown as effective immunotherapeutic agents in preclinical studies. However, in clinical studies, usage of these agents has been limited by low efficacy (utomilumab) and severe hepatotoxicity (urelumab) (96,97). In this thesis study, we reported that the therapeutic doses of SA-4-1BBL did not show any detectable toxicity at the macroscopic level. This result was consistent with previous studies conducted in various preclinical cancer models (31,37,56,58,62). This finding highlighted that SA-4-1BBL can be a safe and efficient alternative to 4-1BB agonists. Treatment of A/J mice with the SA-4-1BBL molecule prevented lung tumor formation. This prevention was significant compared to the control group animals which did not administrate by SA-4-1BBL. Control group mice developed more macroscopic and microscopic tumor nodules than the SA-4-1BBL administered group (Figures 8a, 8b, 9, 10). Importantly, CD4+ T lymphocytes, CD8+ T lymphocytes, and NK cell depletion significantly diminished the antitumoral immunomodulatory and preventive effects of SA-4-1BBL (Figures 14, 15, 17-19). This data suggests that the therapeutic effects of the SA-4-1BBL were conducted by these cell populations. In the CD4+ T cell depletion, macroscopic and microscopic tumor nodules were higher than SA-4-1BBL treated groups without *in vivo* cell depletion. Contrary to CD4+ T cell depletion, the depletion of CD8+ T lymphocytes and NK cells caused a significant increment in microscopic tumor nodules, while did not affect the macroscopic tumor nodule numbers (Figures 11-15, 17-19, 22). These findings could be interpreted as that the immunopreventive activity of SA-4-1BBL molecules is principally led by CD4+ T lymphocytes, accompanying the attendance of CD8+ T lymphocytes and NK cells. Also, these findings showed a cross-interaction between adaptive immunity and

innate immunity. CD4⁺ T lymphocytes are one of the major immune cells that have a critical role in initiating a successful immune response and triggering other immune cells to facilitate effective antibody and immune memory formation. Contrary to CD4⁺ T lymphocytes, CD8⁺ T lymphocytes, and NK cells take a role in the immune response by interacting with the aberrant (malignant or infected) cells. Their importance for antitumoral responses remains unquestionable. The absence of CD8⁺ T lymphocytes and NK cells will drive a compromised immune response against cancer cells, which will lead an aggressive tumorigenesis. As recent work has highlighted (62), treatment with SA-4-1BBL significantly boosted the CD4⁺ naive T lymphocytes and central memory lymphocyte numbers in the lung and draining lymph nodes (Figures 23a, 23b, 23c). It is known that after antigenic exposure, naive CD4⁺ T lymphocytes become activated and further differentiate into various types of effector T lymphocytes (98,99). Effector T lymphocytes can go to infection or tumor areas to eliminate the antigens (100). After the elimination of immune antigen sources, part of the effector T lymphocytes can differentiate into memory T lymphocytes to have an immune repertoire for the next exposure to the same antigenic structures. Memory T cells have a higher proliferation capacity and better and faster immune responses against pathogens and aberrant cells. Since they can be in tissues and persist, besides innate immune cells and natural barriers of the body, they supply a patrol in locations open to infections and foreign materials. Although memory T cell biology and their responses under certain conditions remain not fully determined, they might be the cells that recognized the lung tumor antigens during NNK treatment and were further stimulated by SA-4-1BBL. Besides these findings, SA-4-1BBL treatment diminished the PD-1⁺ CD8⁺ T lymphocytes population, in comparison with SA-4-1BBL non-treated control group (Figure 23d). PD-1 is one of the well-known immune inhibitory receptors expressed on the cell membranes of activated T cell populations, including CD8⁺ T cells. The main function of the PD-1/PD-L1 binding is to regulate the immune responses under chronic antigenic exposures, such can be seen in prolonged/ chronic infections, foreign body reactions, and tumor microenvironments. This chronic exposure induces PD-1 expression in T cells, which leads them to exhaustion. T cell exhaustion serves a great balance against autoimmunity in the body, but it leads to a significant decrease and limitation in T cell's immune capacity. In a significant amount of cancer types, cancer cells use this mechanism to overcome and survive antitumoral immune responses and induce resistance to T-cell attacks. Thus, resulting in a significant reduction in PD-1⁺ CD8⁺ T lymphocytes can be interpreted as SA-4-1BBL treatment can boost the antitumoral immune responses against NNK-induced lung cancer by diminishing the exhaustion of CD8⁺ T lymphocytes. Interestingly, when we ran immune profiling from the mass seen in the mandibula of the CD4⁺ T lymphocyte-depleted group, we saw a high amount of PD-1⁺ CD8⁺ T lymphocytes. This also can reflect that in the metastatic focus of spontaneous lung cancer, cancer cells use T cell exhaustion to escape from immunosurveillance and have a more tolerant tumor microenvironment for tumor progression. Having a depletion of CD4⁺ T lymphocytes might have reduced the effectiveness of the SA-4-1BBL molecule in the prevention of CD8⁺ T cell exhaustion. Nevertheless, it should be noted that without more supporting data, a certain and

complete interpretation of the results that have been mentioned cannot be made. Collectively, our data would seem to indicate that SA-4-1BBL has preventive and immunomodulatory effects during continuous, chronic carcinogen exposure in A/J mice. These results show that immune costimulators, such as SA-4-1BBL, have the potential to be used in immunotherapeutic approaches against cancer. These molecules can take an important role in treating or preventing cancer formation by modulating the immune cell responses. They can be used as an additional and complementary treatment next to immune checkpoint inhibitors. Despite the successful treatment rate of immune checkpoint inhibitors in various cancer types, many patients are unresponsive or resistant to immune checkpoint inhibitor-mediated therapies (101–105). This gives priority to developing new therapeutic approaches to boost efficacy (106,107). Finally, an immune costimulation-based immunotherapy using SA-4-1BBL can give a more precise and targeted approach that prevents various adverse side effects, morbidity, and mortality associated with conventional chemotherapy and radiotherapy in cancer treatment regimens.

6. RESULTS AND SUGGESTIONS

1. Mouse lung tumors and human cancers need to be compared based on the changes in their genes. These investigations can provide a better understanding of the mechanisms of lung tumorigenesis under nicotine products. In future studies, the effectiveness of SA-4-1BBL can be investigated in diverse mouse strains, like xenogeneic models or strains with specific mutation profiles to have a better understanding of the activity of SA-4-1BBL.
2. This thesis study is important to show that SA-4-1BBL can be used to protect from spontaneous cancer formation. However, the focus of this study was not enlightening the mechanism of protective effects of SA-4-1BBL mediated protection. In the next studies, this needs to be evaluated. First, metabolic changes can be evaluated in RNA and protein levels. Later, A/J mice with different gene knockdowns can be used to evaluate the metabolic results of those changes. This can also lead to have a better perspective of the physiology of the 4-1BB/4-1BBL path in normal conditions versus cancer immunology and can be a better target for other novel therapeutic approaches.
3. In this thesis study, we showed that SA-4-1BBL decreased the PD-1+ T lymphocytes and interpreted that SA-4-1BBL treatment can boost the antitumoral immunity against NNK-induced spontaneous lung cancer by diminishing the exhaustion of CD8+ T lymphocytes. However, this interpretation needs to be proved with further analyses. After proving the effect, the same setting of treatment can be performed on mice under anti-PD-1 antibody treatment to see the changes in the activity of SA-4-1BBL. These results can show the feasibility of a combination of immune checkpoint inhibitors plus SA-4-1BBL treatment. On the other hand, we recently published that SA-4-1BBL is an effective molecule to inhibit transplantable tumor types.
4. This study showed that it also has an effect to protect against spontaneous cancer. In the next studies, SA-4-1BBL can be used in various spontaneous cancer models induced by chemical exposures such as polycyclic aromatic hydrocarbon DMBA/TPA (2,4-dimethoxybenzaldehyde/ 12-O-tetradecanoylphorbol 13-acetate) protocols for skin cancer (108) and MCA (3-Methylcholanthrene) for sarcomas (109). With these future studies, we can enlighten the functions of the 4-1BB/4-1BBL path in various cancers and develop novel therapeutic approaches to increase the success rates of immunotherapies in the clinic. This can lead to a paradigm shift in cancer therapies which is still mostly based on conventional chemotherapy and radiotherapy. This change can decrease the morbidity and mortality rates related to therapies and increase the overall survival of cancer patients.

7. REFERENCES

1. Anand P, Kunnumakara AB, Sundaram C, Harikumar KB, Tharakan ST, Lai OS, et al. Cancer is a preventable disease that requires major lifestyle changes. Vol. 25, *Pharmaceutical Research*. Springer New York LLC; 2008. p. 2097–116.
2. Islami F, Goding Sauer A, Miller KD, Siegel RL, Fedewa SA, Jacobs EJ, et al. Proportion and number of cancer cases and deaths attributable to potentially modifiable risk factors in the United States. *CA Cancer J Clin*. 2018 Jan;68(1):31–54.
3. Parkin DM. The global health burden of infection-associated cancers in the year 2002. *Int J Cancer*. 2006 Jun 15;118(12):3030–44.
4. Bouvard V, Loomis D, Guyton KZ, Grosse Y, Ghissassi F El, Benbrahim-Tallaa L, et al. Carcinogenicity of consumption of red and processed meat. *The Lancet Oncology*. Lancet Publishing Group; 2015. p. 1599–600.
5. Clinton SK, Giovannucci EL, Hursting SD. The World Cancer Research Fund/American Institute for Cancer Research Third Expert Report on Diet, Nutrition, Physical Activity, and Cancer: Impact and Future Directions. Vol. 150, *Journal of Nutrition*. Oxford University Press; 2020. p. 663–71.
6. Accessed January 31, 2023 [Internet]. 2023. World Health Organization, Cancer.
7. Siegel RL, Miller KD, Fuchs HE, Jemal A. Cancer statistics, 2022. *CA Cancer J Clin*. 2022 Jan;72(1):7–33.
8. Sung H, Ferlay J, Siegel RL, Laversanne M, Soerjomataram I, Jemal A, et al. Global Cancer Statistics 2020: GLOBOCAN Estimates of Incidence and Mortality Worldwide for 36 Cancers in 185 Countries. *CA Cancer J Clin*. 2021 May;71(3):209–49.
9. Naik PP, Desai MB. Basal Cell Carcinoma: A Narrative Review on Contemporary Diagnosis and Management. Vol. 10, *Oncology and Therapy*. Adis; 2022. p. 317–35.
10. Dillekås H, Rogers MS, Straume O. Are 90% of deaths from cancer caused by metastases? *Cancer Med*. 2019 Sep 1;8(12):5574–6.
11. Siegel RL, Miller KD, Jemal A. Cancer statistics, 2020. *CA Cancer J Clin*. 2020 Jan;70(1):7–30.
12. Nicholson AG, Tsao MS, Beasley MB, Borczuk AC, Brambilla E, Cooper WA, et al. The 2021 WHO Classification of Lung Tumors: Impact of Advances Since 2015. Vol. 17, *Journal of Thoracic Oncology*. Elsevier Inc.; 2022. p. 362–87.
13. Caliman E, Fancelli S, Petroni G, Gatta Michelet MR, Cosso F, Ottanelli C, et al. Challenges in the treatment of small cell lung cancer in the era of immunotherapy and molecular classification. Vol. 175, *Lung Cancer*. Elsevier Ireland Ltd; 2023. p. 88–100.
14. Pao W, Girard N. Review New driver mutations in non-small-cell lung cancer. 2011; Available from: www.thelancet.com/oncologyVol12
15. Leiter A, Veluswamy RR, Wisnivesky JP. The global burden of lung cancer: current status and future trends. Vol. 20, *Nature Reviews Clinical Oncology*. Springer Nature; 2023. p. 624–39.
16. Herbst RS, Baas P, Kim DW, Felip E, Pérez-Gracia JL, Han JY, et al. Pembrolizumab versus docetaxel for previously treated, PD-L1-positive, advanced non-small-cell lung

- cancer (KEYNOTE-010): A randomised controlled trial. *The Lancet*. 2016 Apr 9;387(10027):1540–50.
17. Mamdani H, Matosevic S, Khalid AB, Durm G, Jalal SI. Immunotherapy in Lung Cancer: Current Landscape and Future Directions. Vol. 13, *Frontiers in Immunology*. Frontiers Media S.A.; 2022.
 18. Martin AL, Powell C, Nagy MZ, Innamarato P, Powers J, Nichols D, et al. Anti-4-1BB immunotherapy enhances systemic immune effects of radiotherapy to induce B and T cell-dependent anti-tumor immune activation and improve tumor control at unirradiated sites. *Cancer Immunology, Immunotherapy*. 2023 Jun 1;72(6):1445–60.
 19. Sharma RK, Yolcu ES, Shirwan H. SA-4-1BBL as a novel adjuvant for the development of therapeutic cancer vaccines. Vol. 13, *Expert Review of Vaccines*. 2014. p. 387–98.
 20. Neelapu SS, Locke FL, Bartlett NL, Lekakis LJ, Miklos DB, Jacobson CA, et al. Axicabtagene Ciloleucef CAR T-Cell Therapy in Refractory Large B-Cell Lymphoma. *New England Journal of Medicine*. 2017 Dec 28;377(26):2531–44.
 21. Burt R, Warcel D, Fielding AK. Blinatumomab, a bispecific B-cell and T-cell engaging antibody, in the treatment of B-cell malignancies. *Hum Vaccin Immunother*. 2019 Mar 4;15(3):594–602.
 22. Borghaei H, Paz-Ares L, Horn L, Spigel DR, Steins M, Ready NE, et al. Nivolumab versus Docetaxel in Advanced Nonsquamous Non–Small-Cell Lung Cancer. *New England Journal of Medicine*. 2015 Oct 22;373(17):1627–39.
 23. Gandhi L, Rodríguez-Abreu D, Gadgeel S, Esteban E, Felip E, De Angelis F, et al. Pembrolizumab plus Chemotherapy in Metastatic Non–Small-Cell Lung Cancer. *New England Journal of Medicine*. 2018 May 31;378(22):2078–92.
 24. Hellmann MD, Paz-Ares L, Bernabe Caro R, Zurawski B, Kim SW, Carcereny Costa E, et al. Nivolumab plus Ipilimumab in Advanced Non–Small-Cell Lung Cancer. *New England Journal of Medicine*. 2019 Nov 21;381(21):2020–31.
 25. Kamata-Sakurai M, Narita Y, Hori Y, Nemoto T, Uchikawa R, Honda M, et al. Antibody to cd137 activated by extracellular adenosine triphosphate is tumor selective and broadly effective in vivo without systemic immune activation. *Cancer Discov*. 2021 Jan 1;11(1):158–75.
 26. Siegel RL, Miller KD, Wagle NS, Jemal A. Cancer statistics, 2023. *CA Cancer J Clin*. 2023 Jan;73(1):17–48.
 27. Konstantinou E, Fotopoulou F, Drosos A, Dimakopoulou N, Zagoriti Z, Niarchos A, et al. Tobacco-specific nitrosamines: A literature review. *Food and Chemical Toxicology*. 2018 Aug 1;118:198–203.
 28. Alexandrov LB, Ju YS, Haase K, Van Loo P, Martincorena I, Nik-Zainal S, et al. Mutational signatures associated with tobacco smoking in human cancer. *Science (1979)*. 2016 Nov 4;354(6312):618–22.
 29. Strzelak A, Ratajczak A, Adamiec A, Feleszko W. Tobacco smoke induces and alters immune responses in the lung triggering inflammation, allergy, asthma and other lung diseases: A mechanistic review. Vol. 15, *International Journal of Environmental Research and Public Health*. MDPI AG; 2018.

30. Bitra A, Doukov T, Destito G, Croft M, Zajonc DM. Crystal structure of the m4-1BB/4-1BBL complex reveals an unusual dimeric ligand that undergoes structural changes upon 4-1BB receptor binding. *Journal of Biological Chemistry*. 2019 Feb 8;294(6):1831–45.
31. Schabowsky RH, Elpek KG, Madireddi S, Sharma RK, Yolcu ES, Bandura-Morgan L, et al. A novel form of 4-1BBL has better immunomodulatory activity than an agonistic anti-4-1BB Ab without Ab-associated severe toxicity. *Vaccine*. 2009 Dec 11;28(2):512–22.
32. Barsoumian HB, Yolcu ES, Shirwan H. 4-1BB signaling in conventional T cells drives IL-2 production that overcomes CD4+CD25+FoxP3+ T regulatory cell suppression. *PLoS One*. 2016 Apr 1;11(4).
33. Sharpless NE, DePinho RA. The mighty mouse: Genetically engineered mouse models in cancer drug development. Vol. 5, *Nature Reviews Drug Discovery*. 2006. p. 741–54.
34. Frese KK, Tuveson DA. Maximizing mouse cancer models. Vol. 7, *Nature Reviews Cancer*. 2007. p. 645–58.
35. Ramelow J, Brooks CD, Gao L, Almiman AA, Williams TM, Villalona-Calero MA, et al. The oncogenic potential of a mutant TP53 gene explored in two spontaneous lung cancer mice models. *BMC Cancer*. 2020 Aug 8;20(1).
36. Gordon T, Bosland M. Strain-dependent differences in susceptibility to lung cancer in inbred mice exposed to mainstream cigarette smoke. *Cancer Lett*. 2009 Mar 18;275(2):213–20.
37. Srivastava AK, Dinc G, Sharma RK, Yolcu ES, Zhao H, Shirwan H. SA-4-1BBL and monophosphoryl lipid A constitute an efficacious combination adjuvant for cancer vaccines. *Cancer Res*. 2014 Nov 15;74(22):6441–51.
38. Sharma RK, Yolcu ES, Srivastava AK, Shirwan H. CD4+ T Cells Play a Critical Role in the Generation of Primary and Memory Antitumor Immune Responses Elicited by SA-4-1BBL and TAA-Based Vaccines in Mouse Tumor Models. *PLoS One*. 2013 Sep 16;8(9).
39. Lubet RA, Bnmde MJ, Tmame D, Damle D, Neberf DW, Komi RE. Induction of immunotoxicity by polycyclic hydrocarbons: Role of the Ah locus. Vol. 56, *Arch Toxicol*. 1984.
40. Manenti G, Trincucci G, Pettinicchio A, Amendola E, Scarfò M, Dragani TA. Cis-acting genomic elements of the Pas1 locus control Kras mutability in lung tumors. *Oncogene*. 2008 Sep 25;27(43):5753–8.
41. Kumar B V., Connors TJ, Farber DL. Human T Cell Development, Localization, and Function throughout Life. Vol. 48, *Immunity*. Cell Press; 2018. p. 202–13.
42. Klein Geltink RI, Kyle RL, Pearce EL. Unraveling the Complex Interplay Between T Cell Metabolism and Function. 2018; Available from: <https://doi.org/10.1146/annurev-immunol->
43. Zamarron BF, Chen W. Dual Roles of Immune Cells and Their Factors in Cancer Development and Progression [Internet]. *Int. J. Biol. Sci*. 2011. Available from: <http://www.biolsci.org651>

44. Yan Y, Huang L, Liu Y, Yi M, Chu Q, Jiao D, et al. Metabolic profiles of regulatory T cells and their adaptations to the tumor microenvironment: implications for antitumor immunity. Vol. 15, *Journal of Hematology and Oncology*. BioMed Central Ltd; 2022.
45. Barros L, Piontkivska D, Figueiredo-Campos P, Fanczal J, Ribeiro SP, Baptista M, et al. CD8+ tissue-resident memory T-cell development depends on infection-matching regulatory T-cell types. *Nat Commun*. 2023 Dec 1;14(1).
46. Kaech SM, Cui W. Transcriptional control of effector and memory CD8+ T cell differentiation. Vol. 12, *Nature Reviews Immunology*. 2012. p. 749–61.
47. Joshi NS, Cui W, Chandele A, Lee HK, Urso DR, Hagman J, et al. Inflammation Directs Memory Precursor and Short-Lived Effector CD8+ T Cell Fates via the Graded Expression of T-bet Transcription Factor. *Immunity*. 2007 Aug 24;27(2):281–95.
48. Gajewski TF, Schell SR, Nau G, Fitch FW. Regulation of T-Cell Activation; Differences among T-Cell Subsets. *Immunological Reviews*. 1989.
49. Stam WB, Van Oosterhout AJM, Nijkamp FP. Minireview pharmacologic modulation of Th1- and Th2-associated lymphokine production. *Life Sci [Internet]*. 1993;53(26):1921–34. Available from: <https://www.sciencedirect.com/science/article/pii/002432059390014T>
50. Romagnani S, Del Prete G, Maggi E, Parronchi P, De Carli M, Macchia D, et al. Human TH1 and TH2 Subsets. *Int Arch Allergy Immunol [Internet]*. 2009 Sep 2;99(2–4):242–5. Available from: <https://doi.org/10.1159/000236257>
51. Cua DJ, Tato CM. Innate IL-17-producing cells: The sentinels of the immune system. Vol. 10, *Nature Reviews Immunology*. Nature Publishing Group; 2010. p. 479–89.
52. Korn T, Bettelli E, Oukka M, Kuchroo VK. IL-17 and Th17 cells. Vol. 27, *Annual Review of Immunology*. 2009. p. 485–517.
53. Sakaguchi S, Miyara M, Costantino CM, Hafler DA. FOXP3 + regulatory T cells in the human immune system. Vol. 10, *Nature Reviews Immunology*. 2010. p. 490–500.
54. Chien YH, Meyer C, Bonneville M. $\gamma\delta$ T cells: First line of defense and beyond. Vol. 32, *Annual Review of Immunology*. Annual Reviews Inc.; 2014. p. 121–55.
55. Madireddi S, Schabowsky RH, Srivastava AK, Sharma RK, Yolcu ES, Shirwan H. SA-4-1BBL costimulation inhibits conversion of conventional CD4+ T cells into CD4+FoxP3+ T regulatory cells by production of IFN- γ . *PLoS One*. 2012 Aug 1;7(8).
56. Srivastava AK, Sharma RK, Yolcu ES, Ulker V, MacLeod K, Dinc G, et al. Prime-Boost Vaccination with SA-4-1BBL Costimulatory Molecule and Survivin Eradicates Lung Carcinoma in CD8+ T and NK Cell Dependent Manner. *PLoS One*. 2012 Nov 8;7(11).
57. Sharma RK, Srivastava AK, Yolcu ES, MacLeod KJ, Schabowsky RH, Madireddi S, et al. SA-4-1BBL as the immunomodulatory component of a HPV-16 E7 protein based vaccine shows robust therapeutic efficacy in a mouse cervical cancer model. *Vaccine*. 2010 Aug;28(36):5794–802.
58. Sharma RK, Schabowsky RH, Srivastava AK, Elpek KG, Madireddi S, Zhao H, et al. 4-1BB ligand as an effective multifunctional immunomodulator and antigen delivery vehicle for the development of therapeutic cancer vaccines. *Cancer Res*. 2010 May 15;70(10):3945–54.

59. Vinay DS, Kwon BS. 4-1BB signaling beyond T cells. Vol. 8, Cellular and Molecular Immunology. 2011. p. 281–4.
60. Vinay DS, Cha K, Kwon BS. Dual immunoregulatory pathways of 4-1BB signaling. Vol. 84, Journal of Molecular Medicine. 2006. p. 726–36.
61. Sharma RK, Elpek KG, Yolcu ES, Schabowsky RH, Zhao H, Bandura-Morgan L, et al. Costimulation as a platform for the development of vaccines: A peptide-based vaccine containing a novel form of 4-1BB ligand eradicates established tumors. *Cancer Res.* 2009 May 15;69(10):4319–26.
62. Barsoumian HB, Batra L, Shrestha P, Bowen WS, Zhao H, Egilmez NK, et al. A novel form of 4-1BBL prevents cancer development via nonspecific activation of CD4⁺ T and natural killer cells. *Cancer Res.* 2019 Feb 15;79(4):783–94.
63. Nikitin AY, Alcaraz A, Anver MR, Bronson RT, Cardiff RD, Dixon D, et al. Classification of Proliferative Pulmonary Lesions of the Mouse: Recommendations of the Mouse Models of Human Cancers Consortium [Internet]. Vol. 64, CANCER RESEARCH. 2004. Available from: <http://aacrjournals.org/cancerres/article-pdf/64/7/2307/2523966/2307.pdf>
64. Kim JH, Lee HJ, Kim GS, Choi DH, Lee SS, Kang JK, et al. Inhibitory effects of 7-hydroxy-3-methoxy-cadalene on 4-(methylnitrosamino)-1-(3-pyridyl)-1-butanone (NNK)-induced lung tumorigenesis in A/J mice. *Cancer Lett.* 2004 Sep 30;213(2):139–45.
65. Salehinejad J, Zare-Mahmoodabadi R, Saghafi S, Jafarian AH, Ghazi N, Rajaei AR, et al. Immunohistochemical detection of p53 and PCNA in ameloblastoma and adenomatoid odontogenic tumor. *J Oral Sci.* 2011;53(2):213–7.
66. Croft M. Co-stimulatory members of the TNFR family: Keys to effective T-cell immunity? Vol. 3, Nature Reviews Immunology. European Association for Cardio-Thoracic Surgery; 2003. p. 609–20.
67. Patlolla JMR, Qian L, Biddick L, Zhang Y, Desai D, Amin S, et al. β -escin inhibits NNK-induced lung adenocarcinoma and ALDH1A1 and RhoA/Rock expression in A/J mice and growth of H460 human lung cancer cells. *Cancer Prevention Research.* 2013 Oct;6(10):1140–9.
68. V G, SA K, E S, A C, ML P, M KD, et al. Development of novel approach to diagnostic imaging of lung cancer with ¹⁸F-Nifene PET/CT using A/J Mice treated with NNK. *J Cancer Res Ther (Manch).* 2013 Jun 1;1(4):128–37.
69. Chester C, Ambulkar S, Kohrt HE. 4-1BB agonism: adding the accelerator to cancer immunotherapy. Vol. 65, Cancer Immunology, Immunotherapy. Springer Science and Business Media Deutschland GmbH; 2016. p. 1243–8.
70. Melero I, Sanmamed MF, Glez-Vaz J, Luri-Rey C, Wang J, Chen L. CD137 (4-1BB)-Based Cancer Immunotherapy on Its 25th Anniversary. *Cancer Discov.* 2023 Mar 1;13(3):552–69.
71. Miller RE, Jones J, Le T, Whitmore J, Boiani N, Gliniak B, et al. 4-1BB-Specific Monoclonal Antibody Promotes the Generation of Tumor-Specific Immune Responses by Direct Activation of CD8 T Cells in a CD40-Dependent Manner. *The Journal of Immunology.* 2002 Aug 15;169(4):1792–800.

72. Stabile LP, Kumar V, Gaither-Davis A, Huang EH, Vendetti FP, Devadassan P, et al. Syngeneic tobacco carcinogen-induced mouse lung adenocarcinoma model exhibits PD-L1 expression and high tumor mutational burden. *JCI Insight*. 2021 Feb 8;6(3).
73. Narayanapillai SC, Han YH, Song JM, Kebede ME, Upadhyaya P, Kassie F. Modulation of the PD-1/PD-L1 immune checkpoint axis during inflammation-associated lung tumorigenesis. *Carcinogenesis*. 2020 Nov 1;41(11):1518–28.
74. Elpek KG, Yolcu ES, Franke DDH, Lacelle C, Schabowsky RH, Shirwan H. Ex Vivo Expansion of CD4+CD25+FoxP3+ T Regulatory Cells Based on Synergy between IL-2 and 4-1BB Signaling. *The Journal of Immunology*. 2007 Dec 1;179(11):7295–304.
75. Sharma RK, Yolcu ES, Elpek KG, Shirwan H. Tumor cells engineered to codisplay on their surface 4-1BBL and LIGHT costimulatory proteins as a novel vaccine approach for cancer immunotherapy. *Cancer Gene Ther*. 2010 Oct 11;17(10):730–41.
76. Parkinson CM, O'Brien A, Albers TM, Simon MA, Clifford CB, Pritchett-Corning KR. Diagnostic necropsy and selected tissue and sample collection in rats and mice. *Journal of Visualized Experiments*. 2011 Aug;(54).
77. Van den Broeck W, Derore A, Simoens P. Anatomy and nomenclature of murine lymph nodes: Descriptive study and nomenclatory standardization in BALB/cAnNCrl mice. *J Immunol Methods*. 2006 May 30;312(1–2):12–9.
78. Yu YRA, O'Koren EG, Hotten DF, Kan MJ, Kopin D, Nelson ER, et al. A protocol for the comprehensive flow cytometric analysis of immune cells in normal and inflamed murine non-lymphoid tissues. *PLoS One*. 2016 Mar 1;11(3).
79. Carlino MS, Larkin J, Long G V. Therapeutics Immune checkpoint inhibitors in melanoma [Internet]. Vol. 398, *www.thelancet.com*. 2021. Available from: www.thelancet.com
80. Tran L, Xiao JF, Agarwal N, Duex JE, Theodorescu D. Advances in bladder cancer biology and therapy. Vol. 21, *Nature Reviews Cancer*. Nature Research; 2021. p. 104–21.
81. Díaz-Montero CM, Rini BI, Finke JH. The immunology of renal cell carcinoma. Vol. 16, *Nature Reviews Nephrology*. Nature Research; 2020. p. 721–35.
82. 1 - Datasheet_000646. The Jackson Laboratory A/J mice strain details [Internet]. 2024 [cited 2024 May 5]; Available from: <https://www.jax.org/strain/000646>
83. Li MY, Wang M, Dong M, Wu Z, Zhang R, Wang B, et al. Targeting CD36 determines nicotine derivative NNK-induced lung adenocarcinoma carcinogenesis. *iScience*. 2023 Aug 18;26(8).
84. Hudlikar RR, Sargsyan D, Cheng D, Kuo HCD, Wu R, Su X, et al. Tobacco carcinogen 4-[methyl(nitroso)amino]-1-(3-pyridinyl)-1-butanone (NNK) drives metabolic rewiring and epigenetic reprogramming in A/J mice lung cancer model and prevention with diallyl sulphide (DAS). *Carcinogenesis*. 2022 Feb 1;43(2):140–9.
85. Jiang Y, Zhao J, Zhang Y, Li K, Li T, Chen X, et al. Establishment of lung cancer patient-derived xenograft models and primary cell lines for lung cancer study. *J Transl Med*. 2018 May 22;16(1).

86. Wakamatsu N, Devereux TR, Hong HHL, Sills RC. Overview of the Molecular Carcinogenesis of Mouse Lung Tumor Models of Human Lung Cancer. *Toxicol Pathol.* 2007;35(1):75–80.
87. Jackson EL, Willis N, Mercer K, Bronson RT, Crowley D, Montoya R, et al. Analysis of lung tumor initiation and progression using conditional expression of oncogenic K-ras. *Genes Dev.* 2001 Dec 15;15(24):3243–8.
88. Zhou X, Padanad MS, Evers BM, Smith B, Novaresi N, Suresh S, et al. Modulation of mutant krasG12D-driven lung tumorigenesis in vivo by gain or loss of PCDH7 function. *Molecular Cancer Research.* 2019 Feb 1;17(2):594–603.
89. Kleczko EK, Le AT, Hinz TK, Nguyen TT, Navarro A, Hu CJ, et al. Novel EGFR-mutant mouse models of lung adenocarcinoma reveal adaptive immunity requirement for durable osimertinib response. *Cancer Lett.* 2023 Mar 1;556.
90. Kim DS, Ji W, Kim DH, Choi YJ, Im K, Lee CW, et al. Generation of genetically engineered mice for lung cancer with mutant EGFR. *Biochem Biophys Res Commun.* 2022 Dec 3;632:85–91.
91. Morgan KM, Riedlinger GM, Rosenfeld J, Ganesan S, Pine SR. Patient-derived xenograft models of non-small cell lung cancer and their potential utility in personalized medicine. *Front Oncol.* 2017 Jan 19;7(JAN).
92. Lei P, Ju Y, Peng F, Luo J. Applications and advancements of CRISPR-Cas in the treatment of lung cancer. Vol. 11, *Frontiers in Cell and Developmental Biology.* Frontiers Media SA; 2023.
93. Hartmann O, Reissland M, Maier CR, Fischer T, Prieto-Garcia C, Baluapuri A, et al. Implementation of CRISPR/Cas9 Genome Editing to Generate Murine Lung Cancer Models That Depict the Mutational Landscape of Human Disease. *Front Cell Dev Biol.* 2021 Mar 2;9.
94. Hoffmann D, Rivenson A, Amin S, Hecht SS. Cancer research Clinical 9 Dose-Response Study of the Carcinogenicity of Tobacco-Specific N-Nitrosamines in F344 Rats* * *. Vol. 108, *J Cancer Res Clin Oncol.* 1984.
95. Chung FL, Jiao D. Article in *Cancer Research* [Internet]. 1996. Available from: <http://cancerres.aacrjournals.org/content/56/4/772>
96. Bartkowiak T, Jaiswal AR, Ager CR, Chin R, Chen CH, Budhani P, et al. Activation of 4-1BB on liver myeloid cells triggers hepatitis via an interleukin-27–dependent pathway. *Clinical Cancer Research.* 2018 Mar 1;24(5):1138–51.
97. Qi X, Li F, Wu Y, Cheng C, Han P, Wang J, et al. Optimization of 4-1BB antibody for cancer immunotherapy by balancing agonistic strength with FcγR affinity. *Nat Commun.* 2019 Dec 1;10(1).
98. Wan YY, Flavell RA. How diverse-CD4 effector T cells and their functions. Vol. 1, *Journal of Molecular Cell Biology.* 2009. p. 20–36.
99. Chemin K, Gerstner C, Malmström V. Effector functions of CD4+ T cells at the site of local autoimmune inflammation-lessons from rheumatoid arthritis. *Front Immunol.* 2019;10.
100. Luckheeram RV, Zhou R, Verma AD, Xia B. CD4 +T cells: Differentiation and functions. Vol. 2012, *Clinical and Developmental Immunology.* 2012.

101. Hodi FS, O'Day SJ, McDermott DF, Weber RW, Sosman JA, Haanen JB, et al. Improved Survival with Ipilimumab in Patients with Metastatic Melanoma. *New England Journal of Medicine*. 2010 Aug 19;363(8):711–23.
102. Yang JC, Hughes M, Kammula U, Royal R, Sherry RM, Topalian SL, et al. Ipilimumab (Anti-CTLA4 Antibody) Causes Regression of Metastatic Renal Cell Cancer Associated With Enteritis and Hypophysitis [Internet]. 2007. Available from: <http://journals.lww.com/immunotherapy-journal>
103. Slovin SF, Higano CS, Hamid O, Tejawani S, Harzstark A, Alumkal JJ, et al. Ipilimumab alone or in combination with radiotherapy in metastatic castration-resistant prostate cancer: Results from an open-label, multicenter phase i/ii study. *Annals of Oncology*. 2013 Jul;24(7):1813–21.
104. Brahmer JR, Tykodi SS, Chow LQM, Hwu WJ, Topalian SL, Hwu P, et al. Safety and Activity of Anti-PD-L1 Antibody in Patients with Advanced Cancer. *New England Journal of Medicine*. 2012 Jun 28;366(26):2455–65.
105. Topalian SL, Hodi FS, Brahmer JR, Gettinger SN, Smith DC, McDermott DF, et al. Safety, Activity, and Immune Correlates of Anti-PD-1 Antibody in Cancer. *New England Journal of Medicine*. 2012 Jun 28;366(26):2443–54.
106. Royal RE, Levy C, Turner K, Mathur A, Hughes M, Kammula US, et al. Phase 2 Trial of Single Agent Ipilimumab (Anti-CTLA-4) for Locally Advanced or Metastatic Pancreatic Adenocarcinoma [Internet]. 2010. Available from: <http://journals.lww.com/immunotherapy-journal>
107. Hugo W, Zaretsky JM, Sun L, Song C, Moreno BH, Hu-Lieskovan S, et al. Genomic and Transcriptomic Features of Response to Anti-PD-1 Therapy in Metastatic Melanoma. *Cell*. 2016 Mar 24;165(1):35–44.
108. Neagu M, Caruntu C, Constantin C, Boda D, Zurac S, Spandidos DA, et al. Chemically induced skin carcinogenesis: Updates in experimental models (Review). Vol. 35, *Oncology Reports*. Spandidos Publications; 2016. p. 2516–28.
109. Post SM. Mouse models of sarcomas: critical tools in our understanding of the pathobiology. *Clin Sarcoma Res*. 2012 Dec;2(1).

8. APPENDIX

APPENDIX- 1:

Ethical committee approval of animal use for the thesis project.



Animal Care & Use Committee

McReynolds Hall
Columbia, MO 65211

PHONE 573-882-1746

EMAIL ACUC@Missouri.edu

WEB research.missouri.edu/acqa/

May 21, 2020

Subject: IACUC APPROVAL


Dear Dr. Yolcu:

Your animal use protocol entitled "Exploiting the Immunosurveillance Function of CD137 Immune Checkpoint for Lung Cancer Prevention", 9893, was approved by the ACUC on May 21, 2020 and will expire on May 21, 2023. A *de novo* review of this protocol will need to be performed and approved by the ACUC prior to May 21, 2023 to continue this work.

Jeff Henegar, Ph.D.
Director, Office of Animal
Resources/Animal Care Quality Assurance
University of Missouri-Columbia
Columbia, Missouri 65211

APPENDIX- 2:

Digital receipt of the thesis.



Dijital Makbuz

Bu makbuz ödevinizin Turnitin'e ulaştığını bildirmektedir. Gönderiminize dair bilgiler şöyledir:

Gönderinizin ilk sayfası aşağıda gönderilmektedir.

Gönderen: Ayşe Ece Gülen
Ödev başlığı: IMMUNOMODULATORY EFFECTS OF NOVEL IMMUNE COSTI...
Gönderi Başlığı: IMMUNOMODULATORY EFFECTS OF NOVEL IMMUNE COSTI...
Dosya adı: Ayşe_Ece_Gülen_-_Thesis_28.06.2024.pdf
Dosya boyutu: 4.06M
Sayfa sayısı: 118
Kelime sayısı: 29,439
Karakter sayısı: 175,421
Gönderim Tarihi: 28-Haz-2024 11:00ÖÖ (UTC+0300)
Gönderim Numarası: 2409768900

REPUBLIC OF TURKEY
HACETTEPE UNIVERSITY
FACULTY OF HEALTH SCIENCES

IMMUNOMODULATORY EFFECTS OF NOVEL IMMUNE COSTIMULATOR SA-4-1BBL
IN NIKK-INDUCED LUNG CANCER PRECLINICAL MODEL

Ayşe Ece GÜLEN MD, PhD

TUMOR BIOLOGY AND IMMUNOLOGY PROGRAM
DOCTOR OF PHILOSOPHY THESIS

ANKARA
2024

Copyright 2024 Turnitin. Tüm hakları saklıdır.

APPENDIX- 3:

Originality report of the thesis.

IMMUNOMODULATORY EFFECTS OF NOVEL IMMUNE COSTIMULATOR SA-4-1BBL IN NNK-INDUCED LUNG CANCER PRECLINICAL MODEL

ORJİNALLİK RAPORU

% 17	% 11	% 13	% 2
BENZERLİK ENDEKSİ	İNTERNET KAYNAKLARI	YAYINLAR	ÖĞRENCİ ÖDEVLERİ

BİRİNCİL KAYNAKLAR

1	Ayşe Ece Gulen, Rakesh Rudraboina, Mohammad Tarique, Vahap Ulker, Haval Shirwan, Esma S. Yolcu. "A novel agonist of 4-1BB costimulatory receptor shows therapeutic efficacy against a tobacco carcinogen-induced lung cancer", <i>Cancer Immunology, Immunotherapy</i> , 2023 Yayın	% 6
2	openaccess.hacettepe.edu.tr İnternet Kaynağı	% 1
3	www.jimmunol.org İnternet Kaynağı	% 1
4	www.frontiersin.org İnternet Kaynağı	% 1
5	ir.lib.uwo.ca İnternet Kaynağı	<% 1
6	ir.library.louisville.edu İnternet Kaynağı	<% 1

9. CURRICULUM VITAE

Ayse Ece GULEN (she/her)